Program for the

DFG Rundgespräch Magnetische Hybridmaterialien

Benediktbeuern, September 27th – 29th 2023

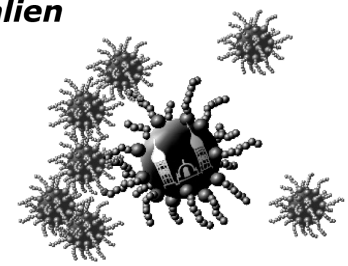

Wedensday, September 27th

14:00 – 14:20	***Opening***	
14:20	**Session 1**	
14:20 – 14:40	S.S. Kantorovich, A. Kuznetsov, D. Mostarac, M. Rosenberg, S. Helbig, D. Suess	*Extended treatment of particle magnetisation in molecular dynamics simulations*
14:40 – 15:00	E. Sese-Sansa, D. Levis, I. Pagonabarraga, G. Liao, S. Klapp	*Active dipolar colloids: interplay of chain formation, phase separation and flocking*
15:00 – 15:20	M. Küster, H. Nádasi, A. Eremin, F. Ludwig	*Magnetic field dependence of the dynamics of BaHF nanoplatelet suspensions*
15:20 – 15:40	P. Bender, L. Rochels, S. Disch	*Shape-induced superstructure formation in concentrated ferrofluids*
15:40	***Coffee break & Posters***	
16:10	***Session 2***	
16:10 – 16:30	D. Kare Gowda, S. Odenbach	*Macroscopic and microscopic properties of thermoplastic polyurethane magnetorheological elastomers*
16:30 – 16:50	N. Boussard, A. Tschöpe	*Restricted mobility of Ni nanorods in agarose hydrogels*
16:50 – 17:10	G.K. Auernhammer	*Measuring internal deformations materials - some new developments*
17:10 – 17:30	P. Schütz, S. Lemich, P. Körner, V. Abetz, B. Hankiewicz	*Synthesis and characterization of magnetoplasmonic $CoFe_2O_4$@Au-NPs in a thermo-responsive polymer matrix*
17:30 – 17:50	M. Kruteva	*Magneto-elastomeric nanocomposites based on polymer-coated nanoparticles*
17:50 – 18:10	J. Landers, S. Zerebecki, S. Salamon, D. Krenz, A. Rabe, S. Reichenberger, S. Barcikowski, H. Wende	*Laser-tuning of magnetic and catalytic properties in spinel-based ferrofluids*
18:10	***Poster Session***	

Thursday, September 28th

approx. 08:30	**Mountain and Alternative Tour**	
approx. 13:30	**Mountain Talks**	
	H. Nádasi, M. Küster, F. Ludwig, ***A. Eremin***	*Ferroelectrics meet ferromagnets: on the way to liquid multiferroic materials*
	S. Lyer, B. Friedrich, M. Dümig, A. Sover, M. Boca, E. Schreiber, J. Band, C. Janko, S. Krappmann, R. Tietze, C. Alexiou	*Magnetic removal of Candida albicans using salivary peptide-functionalized SPIONs*
16:00	**Rundgespräch der Projektleiter**	
19:00	***Workshop dinner***	

Friday, September 29th

8:40	**Session 3**	
8:40 – 9:00	M. Reiche, L. Zentner, D. Borin, T. Becker	*Magnetic field-driven locomotion systems based on magnetoactive elastomers*
9:00 – 9:20	S. Raghavendra Rao, G. Monkman	*Electrical properties of magnetorheological fluids*
9:20 – 9:40	M. Bartunik, J. Kirchner	*Superparamagnetic Nanoparticles in Magnetic Drug Targeting and Molecular Communication*
9:40 – 10:00	T. Viereck, K. Janssen, K. Luenne, M. Schilling, F. Ludwig	*Integrated hyperthermia application and monitoring for localized drug-release in magnetic particle imaging*
10:00 – 10:20	D. Eberbeck, P. Jauch, H. Kratz, F. Wiekhorst, S.G. Mayr	*Migration of magnetic nanoparticles within collagen as an extracellular matrix model: Diffusion vs. magnetic and flow induced steering*
10:20	***Coffee break & Posters***	
10:50	**Session 4**	
10:50 – 11:10	L. Fischer, A. Menzel	*Steering the modes of deformation of soft magnetoelastic actuators by internal structuring*
11:10 – 11:30	P. Gebhart, T. Wallmersperger	*A unified modeling framework for soft and hard magneto-active polymers at the macroscale level*
11:30 – 11:50	D. Romeis, M. Roghani, M. Saphiannikova	*Progress in modeling magneto active elastomers*
11:50 – 12:10	K.A. Kalina, P. Gebhart, J. Brummund, L. Linden, W. Sun, M. Kästner	*Neural network-based multiscale modeling of finite strain magneto-elasticity with relaxed convexity criteria*
12:10	**Closing**	

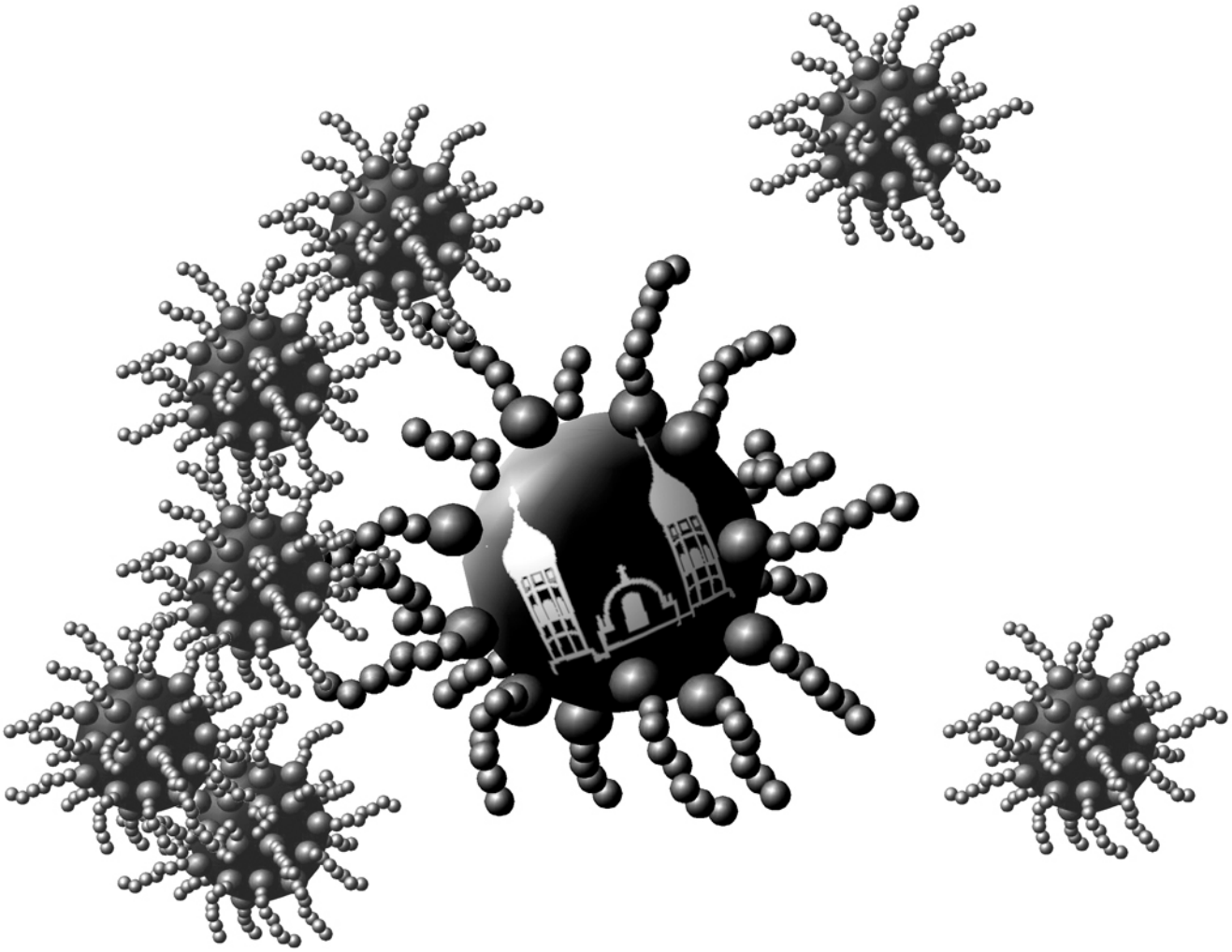

Abstracts

Abstracts

Measuring internal deformations materials - some new developments

G. K. Auernhammer[1]

[1] *Leibniz-Institut für Polymerforschung Dresden eV, Hohe Straße 6, 01069 Dresden, Germany*

For the understanding of basis mechanisms in complex systems under external mechanical load, measuring the internal deformation is often essential. In this presentation I will give some examples on how measuring the internal deformation is possible, including magnetic hybrid materials, dense granular suspensions and viscoelastic polymeric materials. Thereby the focus is on imaging methodologies beyond transmission microscopy [1], including off-focus methods [2] and fast confocal microscopy [3].

Acknowledgments

The presented work is partially supported by the DFG through the SPP 1681 and the SFB 1194 (Project-ID 265191195).

References

[1] Straub, B. B., Schmidt, H., Rostami, P., Henrich, F., Rossi, M., Kähler, C. J., Butt, H.-J., Auernhammer, G. K.; Soft Matter 17, 10090-10100, DOI: 10.1039/D1SM01145F, 2021.

[2] Schmidt, H., Straub, B. B., Sindersberger, D., Bröckel, U., Monkman, G. J., Auernhammer, G. K.: Colloid and Polymer Science 299, 955 -- 967, DOI: 10.1007/s00396-020-04784-4, 2021.

[3] Straub,B. B., Lah,D. C., Schmidt,H., Roth,M., Gilson,L., Butt,H.-J., Auernhammer,G. K.: Review of Scientific Instruments 91 (3), 033706, DOI: 10.1063/1.5122311, 2020.

Superparamagnetic Nanoparticles in Magnetic Drug Targeting and Molecular Communication

M. Bartunik[1], J. Kirchner[1]

[1] *Lehrstuhl für Technische Elektronik (LTE), Friedrich-Alexander-Universität Erlangen-Nürnberg (FAU)*

Superparamagnetic Iron-oxid Nanoparticles (SPIONs)

Superparamagnetic iron-oxid nanoparticles, short SPIONs, consist of a magnetically active core of iron oxide and an application-dependent coating to ensure colloidal stability and often to functionalize the particle surface (see Fig. 1). Particle sizes for medical applications typically vary from 10 nm to 200 nm [1].

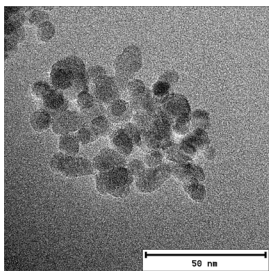

Figure 1: SPION sample, synthesized by the Section for Experimental Oncology and Nanomedicine (SEON) of the University Hospital Erlangen.

The superparamagnetism, i.e. a high susceptibility and no remanence, entails a strong interaction with magnetic fields but avoids particle accumulation in the absence of an external field. Together with their biocompatibility, this makes SPIONs suitable for a wide range of medical applications such as magnetic drug targeting and molecular communication.

SPIONs in Magnetic Drug Targeting

In magnetic drug targeting (MDT), SPIONs are used as carriers for tumor medication. By attracting the particles towards the tumor by use of a strong electromagnet, the fraction of the drug that reaches the target region is increased, thus improving therapeutic success and at the same time reducing adverse effects [2].

SPIONs in Molecular Communication

SPIONs can also be used to carry information, e.g., about insulin dosage between an implanted glucose sensor (transmitter) and an insulin pump (receiver). This is a particular example of molecular communication (MC), where information is transmitted by use of molecules and nano-size particles. MC provides an alternative to conventional data transmission based on electromagnetic fields, in situations where the latter is not applicable, e.g., due to strong signal attenuation, as is the case in the human body [3]. In fact, MDT can be interpreted as a form of MC, both aiming at maximizing the received signal in the target region. In this way, MDT can benefit from methods developed for MC, while SPION-based testbeds provide means for studying MC processes and techniques [4].

SPION Detection

SPION concentrations were initially measured inductively by use of susceptometers, conceived for characterizing material probes. In recent years, we advanced this measurement concept for application in MC and MDT research [5]: An increased temporal resolution allows to investigate time-varying SPION concentrations. Custom-made coils (Fig. 2) enable adaptation of the sensor to different channel geometries; in particular, planar coils facilitate the application in the human body, with blood vessels as transmission channels [6]. Furthermore, by placing several sensors around the channel, information about the SPION distribution across the channel cross-section is obtained [7].

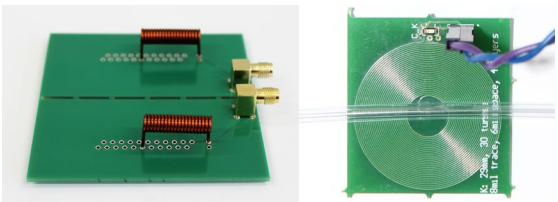

Figure 2: Inductive sensors with cylindrical and flat coil.

An alternative measurement approach is the use of capacitive sensors (see Fig. 4), which exhibit a larger signal-to-noise ratio than in the inductive approach but slower responses [8]. Furthermore, they promise

a reduced sensitivity to electromagnetic interference.

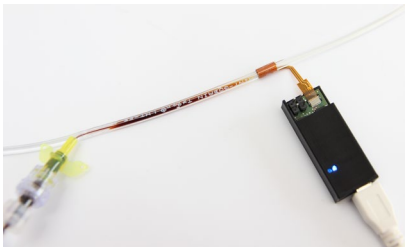

Figure 3. Injection of SPIONs into a silicone tube and capacitive sensor.

SPION Steering

The feasibility of particle steering tube branchings has been demonstrated experimentally by several research groups [9,10]. The results from our measurements with a custom-made electromagnet at a branching are shown in Fig. 4 [7]. The difference of susceptibility, hence of SPION concentration, between the two channels behind the branching is shown in relation to the applied magnetic flux density, for different flow velocities.
For magnetic flux densities < 300 mT, the setup successfully directs more particles into the target branch, with the effect increasing with increasing magnetic field. A larger field strength, however, causes an accumulation of the particles in the vicinity of the electromagnet and thus diminishes the steering effect. Both effects are more pronounced the smaller the fluid flow is. Hence, an optimum has to be found between steering and avoidance of SPION accumulation.

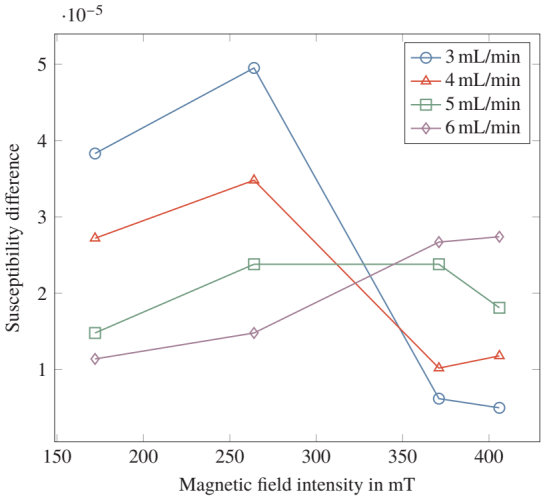

Figure 4. Results of the SPION steering setup.

What's Next?

In conclusion, both animal studies and lab measurements have demonstrated the feasibility and effectiveness of MDT and MC, two related approaches highly desired for medical use. For optimal results, the steering/communication setup has to be adapted to the geometry and flow profile of the individual channel. However, both a systematic investigation of the physical and particularly biological processes, i.e., a comprehensive model, and algorithms for optimizing the parameters of the steering setup with respect to the SPION concentration in the target region are still missing. Such a model plus optimization algorithm has to capture the full complexity of the channel, with respect to both the vascular structure and the involved bio-physical processes, and at the same time, be able to computationally handle such complex models. If these challenges can be solved, MDT and MC will improve cancer treatment and open up new applications of SPIONs in medical care.

References

[1] M. Mahmoudi et al., "Superparamagnetic iron oxide nanoparticles (SPIONs): development, surface modification and applications in chemotherapy", Adv. Drug Delivery Rev. 63(1-2), 24–46, 2011.

[2] R. Tietze et al., "Efficient drug-delivery using magnetic nanoparticles–biodistribution and therapeutic effects in tumour bearing rabbits", Nanomed. Nanotechnol. Biol. Med. 9(7), 961–971, 2013.

[3] T. Nakano, "Molecular communication", Cambridge: Cambridge University Press, 2013.

[4] S. Lotter et al., "Experimental Research in Synthetic Molecular Communications", IEEE Nanotechnol. Mag. 17(3), 42-65, 2023.

[5] M. Bartunik, G. Fischer, J. Kirchner, "The Development of a Biocompatible Testbed for Molecular Communication with Magnetic Nanoparticles", IEEE Trans. Mol. Biol. Multi-Scale Commun. 9(2), 179-190, 2023.

[6] M. Bartunik et al., "Planar coils for detection of magnetic nanoparticles in a testbed for molecular communication", Proc. 9th ACM Int. Conf. Nanoscale Comput. Commun. (NANOCOM '22), Barcelona, Spain, Oct. 5–7, 2022.

[7] M. Bartunik, "Practical Molecular Communication: The Development of two Testbeds," Dissertation, Friedrich-Alexander-Universität Erlangen-Nürnberg (FAU), 2023 (to be publ.).

[8] M. Bartunik, J. Reichstein, J. Kirchner, "Capacitive Sensing for Magnetic Nanoparticles in Molecular Communication", 2022 IEEE Int. Instr. Meas. Technol. Conf. (I2MTC), Ottawa, Canada, May 16–19, 2022.

[9] K. Gitter, S. Odenbach, "Experimental investigations on a branched tube model in magnetic drug targeting", J. Magn. Magn. Mater. 323(10), 1413–1416, 2011.

[10] A. K. Hoshiar et al., "Swarm of magnetic nanoparticles steering in multi-bifurcation vessels under fluid flow", J. Micro-Bio. Robot 16, 137–145, 2020.

Shape-induced superstructure formation in concentrated ferrofluids

P. Bender[1], L. Rochels[2;3], S. Disch[2;3]

[1]*Heinz Maier-Leibnitz Zentrum (MLZ), Technische Universität München, Germany*
[2]*Department für Chemie, Universität zu Köln, Germany*
[3]*Institut für Anorganische Chemie und Center for Nanointegration CENIDE, Universität Duisburg-Essen, Germany*

The response of magnetic nanoparticles (MNPs) to applied static and dynamic magnetic fields is the subject of intense research in view of its fundamental technological importance, e.g., for medical applications such as imaging and magnetic hyperthermia [1], or sensor applications [2]. The field-assisted self-organization of shape-anisotropic nanoparticles in dispersions is further desired for liquid crystalline or optically anisotropic materials [3] and as a prerequisite for self-organization into long range ordered arrangements [4]. The heating behavior of MNPs in AC magnetic field is largely influenced by interactions arising from nanoparticle aggregation [5]. A detailed understanding of interparticle interactions in colloidal dispersion is therefore crucial for the advancement of magnetic hyperthermia.

A variety of nanoparticle arrangements has been observed for colloidal dispersions of spherical MNPs with different particle sizes, ranging from reversible chain-formation [6] to extended columns [7], or even crystalline arrangements of MNPs [8]. The strong structure-directing influence of the particle shape on the symmetry of mesocrystalline arrangements has been studied in detail for nanocubes with a varying degree of corner truncation [9–11]. In this contribution, we present the influence of the particle shape on the superstructure formation in concentrated colloidal dispersions.

The nanoparticles under study consist of maghemite (γ-Fe_2O_3) nanospheres and nanocubes with a 9 nm diameter and 8.5 nm edge length, respectively, and excellent monodispersity with lognormal size distributions of 5.5(1) and 7.2(2) % FWHM.

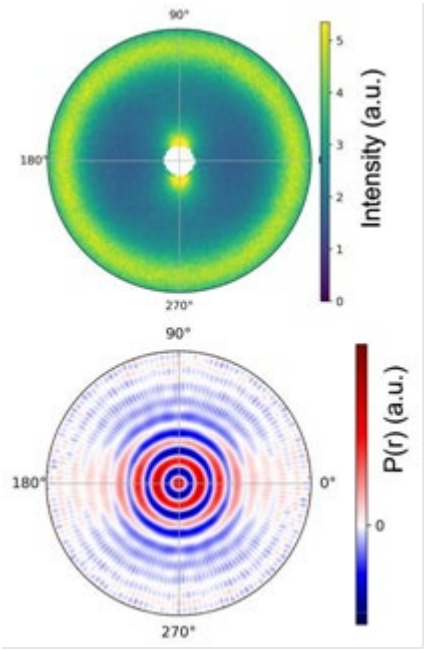

Figure 1. a) SANS pattern of nanocubes in a 1.5 T magnetic field (applied horizontally) b) 2D pair distance distribution derived by SVD [14].

The integral nanoparticle moment of the samples is very similar, with a stronger degree of surface-near spin disorder in the nanocubes [12]. Despite the similar particle size, magnetic moment, and volume concentration (>5 vol-%), we observe a significantly distinct aggregation behavior of nanospheres and nanocubes using Small-Angle Neutron Scattering (SANS).

Both samples reveal a short range ordered hard spheres interaction potential with random orientation towards an applied magnetic field that is observed as ring-shaped correlation peak in the 2D SANS detector (Fig. 1a).

The particle-particle distances derived from the peak position are significantly smaller than observed in ordered assemblies of the same particles [9, 10], and a preference of face-to-face orientation of the nanocubes is likely. The distinct aggregation behavior of the cubic nanoparticles is expressed in a much stronger correlation peak which exhibits an unusual field-dependence suggesting field-induced order and structural rearrangement. Additionally, a directionally anisotropic scattering contribution observed in the lower Q range indicates oriented attractive interparticle interactions of the nanocubes. This becomes visible in the 2D pair distance distribution function extracted from the 2D scattering pattern using the Singular Value De-composition approach (Fig. 1b) [13], which we interpret as an internally nearly isotropic superstructure which extends anisotropically in the field direction [14].

In our contribution, we give a detailed account on the impact of nanoparticle shape and size on the interparticle correlations in colloidal dispersions of maghemite nanoparticles. Particular emphasis is on the aggregation behavior of cuboidal particles in highly concentrated dispersions. The field-dependent arrangement into mesocrystalline assemblies and their geometric orientation will be dis-cussed as observed by field-dependent small-angle scattering experiments.

Acknowledgments

We acknowledge the provision of beam time at the instrument D22 at the Institut Laue-Langevin, Grenoble, France, and the CoSAXS beamline at MAX IV. Albrecht Wiedenmann and Tomas Plivelic are acknowledged for their support in data acquisition at D22 and CoSAXS, respectively.

References

[1] Q. A. Pankhurst et al., J. Phys. D: Appl. Phys. 36, R167 (2003).
[2] D. T. N. Chen et al., Annual Review of Condensed Matter Physics 1, 301 (2010).
[3] G. M. Whitesides, B. Grzybowski, Sci-ence 295, 2418 (2002).
[4] A. Ahniyaz et al., Proc. Natl. Acad. Sci. U.S.A. 104, 17570 (2007).
[5] I. Andreu, A. Urtizberea, E. Natividad, Nanoscale 12, 572 (2020).
[6] N. Nandakumaran et al., Adv. Mater. 33, 2008683 (2021).
[7] M. Klokkenburg et al., Phys. Rev. E 75, 051408 (2007).
[8] Z. Fu et al., Nanoscale 8, 18541 (2016).
[9] S. Disch, E. Wetterskog et al., Nano Letters 11, 1651 (2011).
[10] S. Disch et al., Nanoscale 5, 3969 (2013).
[11] E. Wetterskog et al., Nanoscale 8, 15571 (2016).
[12] S. Disch et al., New J. Phys. 14, 013025 (2013).
[13] P. Bender et al., Acta Cryst. A 75, 766 (2019).
[14] P. Bender, S. Disch et al., J. Appl. Cryst. 55, 1613 (2022).

Magnetic polymer containing liquid metal

D.Y. Borin, R.E.G. Houghton, C. Lehmann, S. Odenbach

Technische Universität Dresden, 01069 Dresden, Germany

By combining an elastic polymer matrix with a specific type of filler, it is possible to create materials with modified and/or controllable properties. For example, an elastomer filled with magnetic microparticle powder is called a magnetorheological elastomer (MRE). The physical properties of MREs are actively controlled by an external magnetic field. If the filler powder is magnetically hard, the so-called passive tuning of the material properties is provided by the pre-magnetisation of the composite, while active control remains possible [1].

Recently, numerous studies have been carried out on the physical properties of mixed polymer-liquid metal composites, opening up perspectives for their use in various types of applications [2]. Furthermore, it has been proposed to combine such type of composite with magnetic soft filler, towards liquid metal based magnetorheological elastomer [3].

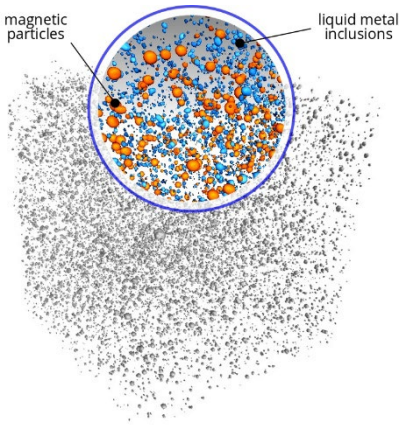

Figure 1. Rendered 3D μCT image of the composite filled with NdFeB-alloy micropartciles and liquid GaInSn alloy droplets.

In the present work, we have fabricated and experimentally investigated a magnetic elastic composite based on a polydimethylsiloxane matrix and a mixed filler consisting of solid and liquid phases (Figure 1). As the solid phase we used a powder of magnetic hard microparticles. As the liquid phase, a liquid at room temperature eutectic GaInSn alloy was used. Mechanical stirring of the liquid metal in the polymer matrix leads to an emulsion in which liquid metal microdroplets are the dispersed phase. A soft elastomer with corresponding inclusions is obtained by subsequent polymerisation. Regardless of the concentration and type of filler, the material is an insulator. Both types of filler increase the relative permittivity to the same extent, whether the filler is solid, liquid or mixed. It is the total concentration of filler that matters. At the same time, the liquid metal inclusions reinforce the polymer matrix to a much lesser extent, allowing the composite to remain softer (Figure 2).

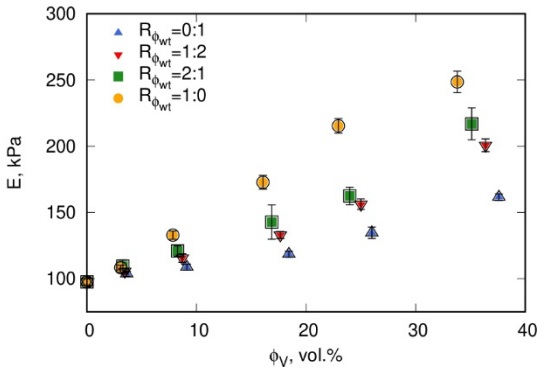

Figure 2. Elastic modulus of the composite as a function of the mixed filler total volume concentration. Results are given for different mass ratios of solid particles to liquid metal.

The presence of the magnetic hard filler allows functionalisation of the material by tuning its residual magnetisation. The result is a soft elastic magnet with increased relative permeability compared to the unfilled matrix. The pre-magnetisation has no significant effect on the mechanical and electrical properties studied, while the liquid metal inclusions do not affect the residual magnetisation of the composite. A specific study is required to evaluate the possibility of active control of composite properties by means of an external magnetic field.

References

[1] D. Borin et al., Arch. Ap. Mech. 89 (2019) 105.
[2] M. D. Bartlett et al., Adv. Mat. 28 (2016) 3726.
[3] G. Yun et al. Nature Comm., 10 (2019) 1300.

Restricted mobility of Ni nanorods in agarose hydrogels

N. Boussard, A. Tschöpe

Universität des Saarlandes, Experimentalphysik, Campus E2 6, 66123 Saarbrücken

Introduction

Hydrogels are biphasic materials consisting of a three-dimensionally linked polymer network and a liquid that fills the interstices. The liquid provides a medium for the transport of embedded particles, which is, however, more or less hindered by the elastic network.

Agarose hydrogels have large pore sizes in a range comparable to the typical length of Ni nanorods [1]. The aim of the present study was to investigate how the rotational and translational motion of magnetic nanorods in agarose hydrogels is constrained by the semiflexible polysaccharide scaffold.

Methods

Ni nanorods of different length (≈100-600 nm) were prepared by the AAO-template method and processed to stable aqueous colloidal dispersions [2,3]. Basic physical properties of the Ni nanorods, such as the length distribution P(L), mean magnetic moment ⟨m⟩ and hydrodynamic layer thickness Λ_{hyd} were obtained by transmission electron microscopy (TEM), static- (SFOT) [4] and oscillating field (OFOT) [5] optical transmission measurements, respectively.

Agarose was dissolved at various concentrations (0.3-1.0 wt.%) in distilled water at 95°C and mixed with the preheated nanorod colloids. The mixtures were subjected to a homogeneous magnetic field (10 mT) in the sol state and during gelation to align the nanorods. For measurements of the shear modulus, pure agarose gels were formed in situ in the CP measuring system of a MARS II rheometer. The correlation lengths ξ were obtained from spectrophotometric turbidity measurements of pure agarose gels using the characteristic relation $\alpha(\xi)$ of the wavelength exponent in the optical extinction $E \propto \lambda^{\alpha}$ [6].

Results

The first experiment addressed the rotational degree of freedom of Ni nanorods in agarose hydrogels, focusing on the accessible angular range. Assuming rotational symmetry, the second moment of the nanorod orientation distribution function $x=\langle\cos 2\theta\rangle$ could be determined from the optical transmission of linearly polarized light. Starting from the initial alignment $(x=1)$ the alignment parameter x relaxed within 100 ms after switching off the field to a steady-state value x_r in the range between $x_r=1/3$ (isotropic) and $x_r=1$ (uniaxial). The final state correlated qualitatively with the ratio $\langle L\rangle/\xi$, i.e., short rods in an open mesh were assuming a nearly isotropic distribution whereas long rods in narrow meshes remained fixed in their parallel alignment. A quantitative model was derived by adapting the Edwards tube model. The topological constraint on the rotational motion of the nanorods, imposed by the agarose network, was approximated by a confining tube of diameter d_t. The optical extinction of representative ensembles of nanorods with random center positions and orientations consistent with the geometric constraint was simulated. In addition to $\langle L\rangle$ and ξ, the distribution $P(L)$ and the mean hydrodynamic diameter $D_{hyd}=D_{TEM}+2\Lambda_{hyd}$, known from TEM and OFOT characterization, were also included in the model. Two unknown model parameters were introduced, the ratio $a=d_t/\xi$ between tube diameter and correlation length, and the scatter parameter σ_ξ of a lognormal distribution $P(\xi)$ for the correlation length. The experiments systematically showed larger scatter at lower agarose concentrations, as reflected by larger error bars in Fig. 1. A weighted χ^2-fit of the model accounting for unequal uncertainties was systematically below these data. This could be due to larger inhomogeneities in the network structure [1] and nanorod

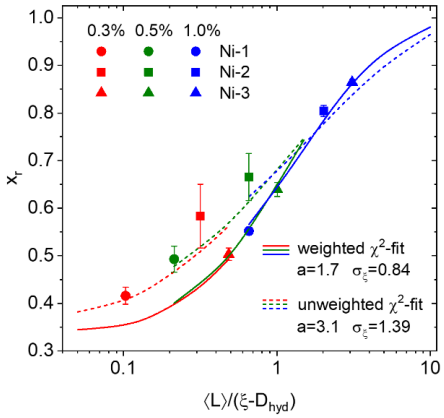

Figure 1. Alignment parameter x_r of Ni nanorods after relaxation in agarose hydrogels as function of the ratio ‹L›/(ξ–D_{hyd}). The transition from a nearly isotropic distribution (x_r=1/3) to a fixed uniaxial alignment (x_r=1) could be well described by the tube model. The uneven uncertainties (error bars) had a large effect on the results obtained from weighted vs. unweighted χ^2-fits.

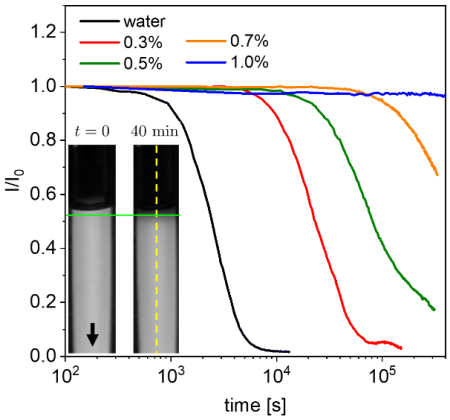

Figure 2. Time-dependent intensity during magnetophoresis of nanorods in water and agarose hydrogels of different concentration. The intensity was measured at a position 200 µm below the upper phase boundary (insert, green line) in the center of the capillary.

distribution after phase separation at low concentration. Macroscopic translational motion of the nanorods in agarose hydrogels was investigated by magnetophoresis. The textured homogeneous nanorod/agarose mixtures were prepared in glass capillaries and placed in a field gradient (Halbach magnet) of *5.5 T/m*. Two crossed polarizers were used to block the backlight whereas the nanorods became clearly visible due to their linear dichroism. Intensity profiles along the capillary center were obtained from digital images. The nanorods, homogeneously distributed in the initial state, moved in the field gradient and the region below the phase boundary was continuously depleted, Fig.2. This process could be monitored by measuring the intensity as function of time at a fixed position. The experiments revealed similar but significantly shifted profiles of the time-dependent intensity. These results confirmed long-range ($\Delta z \approx 850 \times \langle L \rangle$) translational motion of nanorods in agarose hydrogels. The observed shift with increasing agarose concentration corresponded to a reduction in mean drift velocities by 1-2 orders of magnitude.

Conclusion and Outlook

For the combinations of nanorod length and agarose concentration of this study, the Ni nanorods showed the transition from nearly free mobility to fixation. The ferromagnetism of the nanorods will be used in future studies to investigate the anisotropy of mobility and the effect of external stimulation.

References

[1] I. Jayawardena, P. Turunen, B. C. Garms, A. Rowan, S. Corrie, L. Grondahl, Mater. Adv. 4 (2023) 669.
[2] P. Bender, A. Günther, A. Tschöpe, and R. Birringer, JMMM 323 (2011) 2055.
[3] M. Gratz, and A. Tschöpe, Macromol. 52 (2019) 6600.
[4] F. Krämer, M. Gratz, and A. Tschöpe, J. Appl. Phys. 120 (2016) 044301.
[5] A. Tschöpe, K. Birster, B. Trapp, P. Bender, and R. Birringer, J. Appl. Phys. 116 (2014) 184305.
[6] P. Aymard, D. R. Martin, K. Plucknett, T. J. Foster, A. H. Clark, I. T. Norton, Biopolym. 59 (2001) 131.

Overview: A comprehensive characterization and description of the properties of magnetic alginate hydrogels.

Ch. Czichy, St. Odenbach

Chair of Magnetofluiddynamics, Measuring and Automation Technology, TU Dresden, 01069 Dresden, Germany

In the field of tissue engineering, a central issue is the manufacture of patient-specific implants. One possibility lies in additive manufacturing such as extrusion printing. Accordingly, there are many different approaches. A novel approach in the "IndivImp" project was the design of magnetic scaffolds, which are specifically deformed with the application of a magnetic field [1].
In this context, comprehensive studies were carried out on the material properties such as the Young's modulus [2], on the deformation behavior, time behavior, particle structure and ageing behavior [1]. Likewise, two test rigs were created, one allowing investigation in the µCT [1] and the second the cyclic, contactless stimulation of samples [3].
With this contribution we would like to give an overview of the results in Fig. 1 and look ahead to future research.

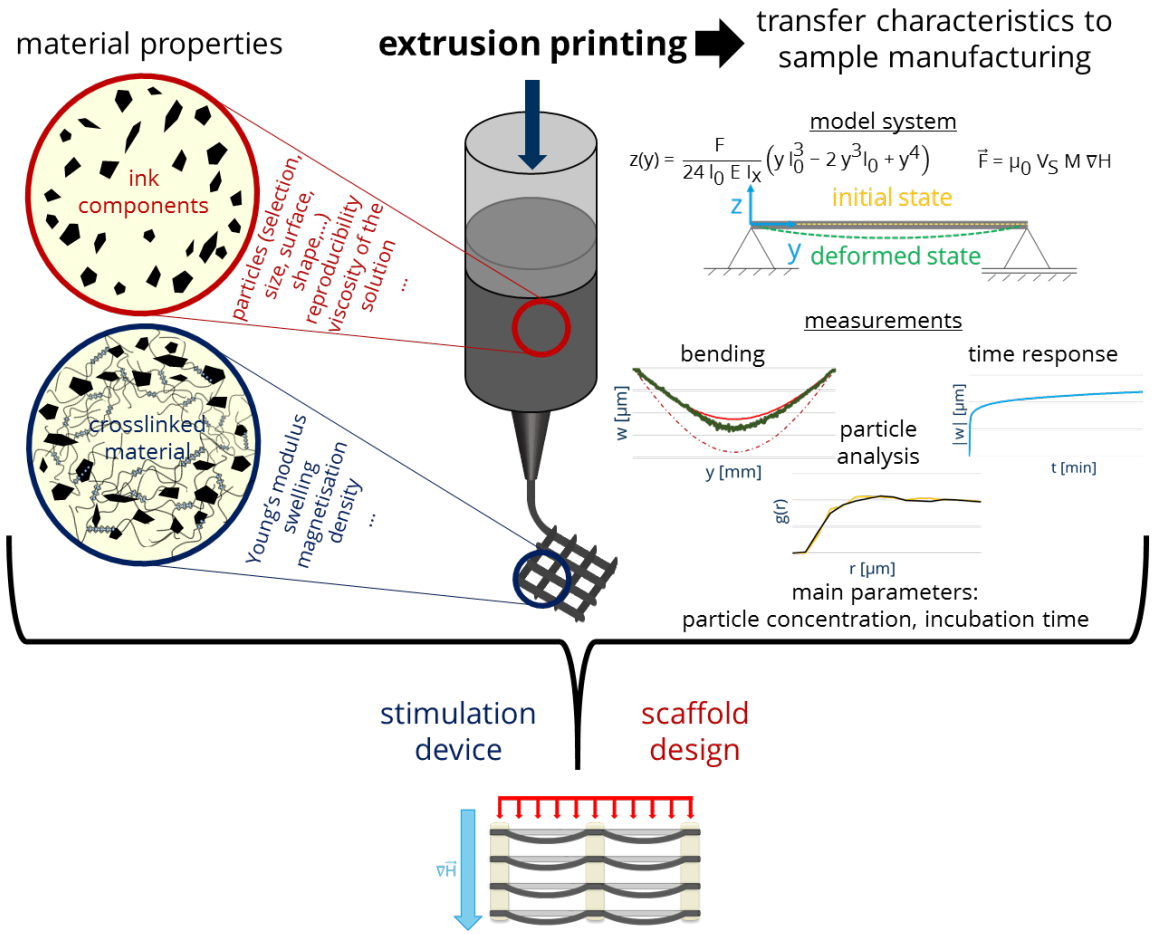

Figure 1. Overview of the investigations regarding magnetic alginate hydrogels für extrusion printing in the field of tissue engineering

Outlook

During the research, several new questions arose and other areas of the manufacturing process, cross-linking and storage, and ageing behavior require further, more in-depth consideration. This applies, for example, to the time response, for which a separate test set-up is needed, as well as for investigations regarding cyclic deformation. An interesting topic is e.g. the influence of a magnetic field, which is either applied during the printing process or when the strands are deposited before cross-linking. Also of interest is the scaffold design, the stimulation of the cells and their reaction to stimulation, printing process, particle content and magnetic field. Ideas and open questions are presented and open the dialogue for discussions, suggestions and further project ideas.

Acknowledgments

The authors would like to thank the European Social Fund (ESF) and the Free State of Saxony for financial support of this project in the course of the ESF Young Researchers Group IndivImp at TU Dresden.
Financial support from the Deutsche Forschungsgesellschaft (DFG) for the Research Training Group 1865 Hydrogel-based Microsystems is also gratefully acknowledged.

References

[1] Spangenberg, Kilian, Czichy, Ahlfeld, Lode, Günther, Odenbach, Gelinsky: Bioprinting of Magnetically Deformable Scaffolds", ACS Biomater. Sci. Eng 2, 2021.

[2] Czichy; Spangenberg; Günther, Gelinsky, Odenbach: "Determination of the Young's modulus for alginate-based hydrogel with magnetite-particles depending on storage conditions and particle concentration" Journal of Magnetism and Magnetic Materials 2020, 501, 166395.

[3] Czichy; Kilian, Wang, Günther, Lode, Gelinsky, Odenbach: "CyMAD bioreactor: a cyclic magnetic actuation device for magnetically 1 mediated mechanical stimulation of 3D bioprinted hydrogel scaffolds" Journal of the mechanical behaviour of biomedical materials, 2022.

Migration of magnetic nanoparticles within collagen as an extracellular matrix model: Diffusion vs. magnetic and flow induced steering

D. Eberbeck[1*], P. Jauch[2*], H. Kratz[3], F. Wiekhorst[1], S.G. Mayr[2]

[*] *contributed equally*
[1] *Physikalisch-Technische Bundesanstalt, Berlin, Germany*
[2] *Division of Surface Physics, Department of Physics and Earth Sciences, University of Leipzig and Leibniz Institute of Surface Engineering (IOM), Permoserstr. 15, 04318, Leipzig, Germany*
[3] *Department of Radiology, Charité-Universitätsmedizin Berlin, Corporate Member of Freie Universität Berlin and Humboldt-Universität zu Berlin, D-10117 Berlin, Germany*

The constant development, research and possible application of new nanoparticle systems urgently requires standardizable and reproducible test systems to predict *in vivo* behavior. In this study, the interaction of the extracellular matrix component collagen with magnetic nanoparticles (MNP) with and without post –synthesis PEG coating was analyzed by quantification of the retention of the MNP after passing through a column of collagen. PEG (Polyethylene glycol) is a flexible, water soluble polymer, which improves blood half live of SPIOs *in vivo* [1] [2].
Here we will characterize the two MNP-systems with respect to its opsonization behavior, i.e., its capability of binding biomolecules as a potential prerequisite of binding to the collagen matrix, applying Alternating Current Susceptibility (ACS) revealed to be a powerful tool for the estimation of the change of the hydrodynamic diameter of MNP. For the sake of the estimation of the thickness of the primary shell we analyzed ACS and M(H) data by a simultaneous fit of a model (Figure 1) which regards the apparent multi-domain structure of the 2 Multicore-MNP (MCMNP) systems, (i) coated with carboxymethyldextran (M*COO) and (ii) additionally coated with mPEG-amine with a molecular weight of 10 kDa (M*CONH-PEG), phenomenologically, yielding core size distribution, the thickness of the primary coating layer and the thickness of the opsonisation layer, built after incubation of the MNP in bovine serum albumin and fetal calf serum (FCS) (Table 1).
The results show a clear opsonisation of M*COO in BSA with a thickness consistent with a mono-layer of albumin (molecule size is about 4 nm), while no significant increase of the particle's hydrodynamic diameter was observed for M*CONH-PEG which has a larger thickness of primary coating, δ_s, due to the PEG (Figure 1b).

Table 1. Mean volume diameter, $d_{v,c}$, and dispersion parameter, σ_c, of the core sizes and thickness of the polymeric shell, δ_s, as well as the thickness of the adsorbed corona, δ_{cor}, of the investigated MNP systems.

parameter	M*COO	M*CONH-PEG
$d_{v,c}$/nm	30.0(2)	35.6(2)
σ_c	0.196(7)	0.124(5)
δ_s/nm	2.8(4)	20.5(7)
δ_{cor}/nm	4.2(2)	0.5(7)

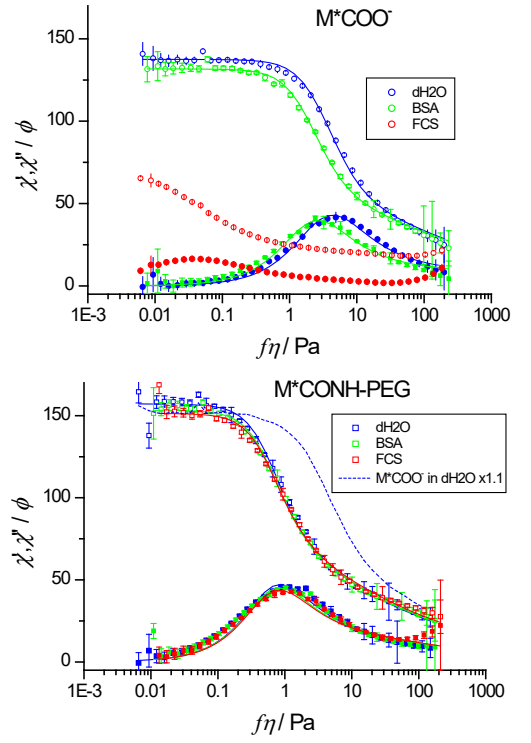

*Figure 1. ACS-data (symbols) and best fit curves (lines) for a) M*COO and b) M*CONH-PEG, dispersed in indicated media, demineralized water (dH2O), BSA and FCS.*

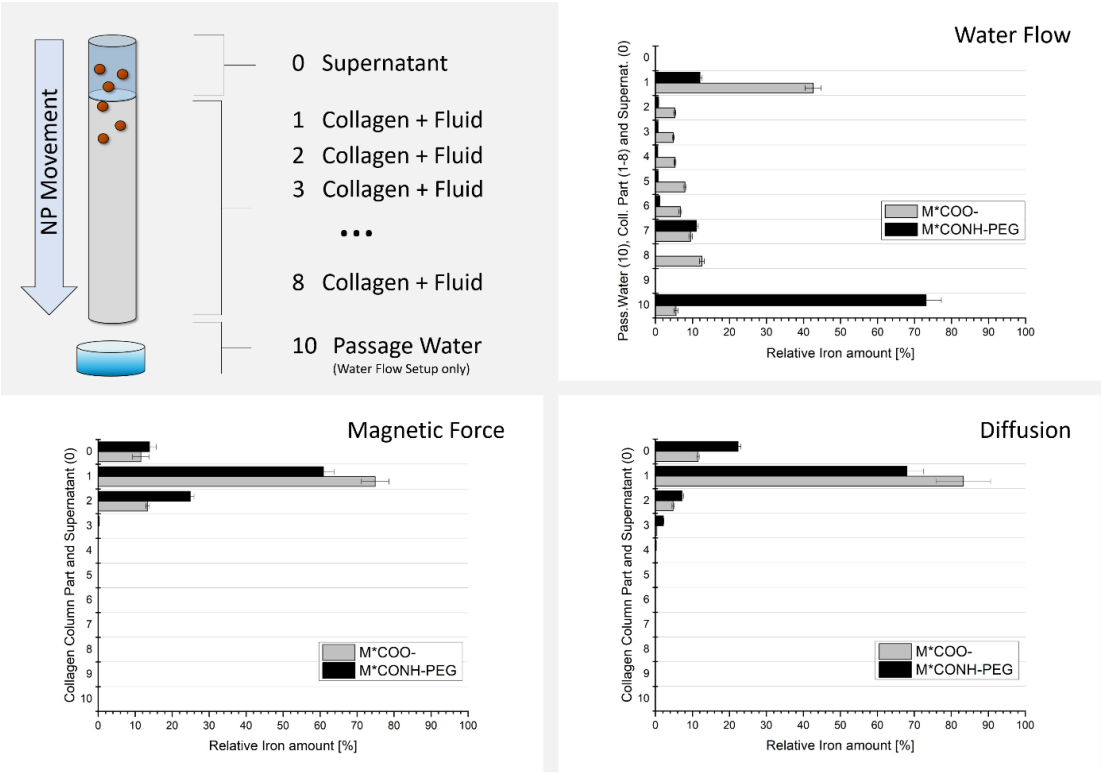

Figure 2. Schematic draw of the collagen column housed by a straw (upper left) and the relative amount of MNP found within the pieces of the collagen column (numbered by 1-10) following the downward movement of the MNP driven by diffusion only, additional magnetic force, and by water flow. The presented iron amount is the sum of MNP found in the collagen parts and the released liquid while sectioning of the collagen column. "Passage Water" denotes the MNP which were collected beneath the column.

The hydrodynamic diameter of M*CONH-PEG does not increases even in FCS which contains a rich variety of biomolecules obviously evoking a cross linkage of M*COO which results in a dramatic increase of hydrodynamic diameters (Figure 1a).
Collagen hydrogels were prepared directly within a straw. The MNP dispersion was put on top of this collagen column. Following 48 h the MNP could penetrate into the collagen column by diffusion ("diffusion"), additionally by an applied magnet field gradient ("Magnetic Force") and by an applied water flow ("Water Flow"). The amount of MNP within the pieces of sectioned collagen column was quantified by Magnetic Particle Spectroscopy (MPS). By magnetic force 2-3 times more MNP reach the deeper part of the column in comparison to pure diffusion (Figure 2). Note, 1st part may be strongly influenced by not penetrated, surface bound MNP. M*CONH-PEG shows an about 2-fold higher penetration than M*COO. While in "Diffusion" and "Magnetic Force"-setup the MNP do not penetrate deeper than to the 3rd piece, the MNP were strongly pushed downwards by the external water flow. Also in this set-up the M*COO particles bind to a much larger amount to the collagen than M*CONH-PEG.
Based on the opsonisation results we expected a larger difference between the two MNP-systems. We discuss the binding of M*CONH-PEG to collagen fibrils in the context of a mushroom-like structure of the PEG on the M*CONH-PEG particles.

Acknowledgments

This work was supported by the DFG priority program 1681.

References

[1] A. P. Khandhar et al., Nanoscale 9, 1299 (2017).

[2] H. Kratz et al., Nanomaterials 9, 1466 (2019).

[3] S. Schöttler et. al., Nat. Nanotechnol. 11, 372 (2016).

Measuring internal deformations materials - some new developments

A. Feoktystov[1*], T. Köhler[1,2,3], O. Petracic[2], E. Kentzinger[2], T. Bhatnagar-Schöffmann[2,3,4], M. Feygenson[5,6], N. Nandakumaran[2,3], J. Landers[7], H. Wende[7], A. Cervellino[8], U. Rücker[2], A. Kovács[4], R.E.Dunin-Borkowski[4], Th. Brückel[2,3]

[1]*Forschungszentrum Jülich GmbH, JCNS at MLZ, Garching, Germany*
[2]*Forschungszentrum Jülich GmbH, JCNS-2 and PGI-4, JARA-FIT, Jülich, Germany*
[3]*Lehrstuhl für Experimentalphysik IV C, RWTH Aachen University, Aachen, Germany*
[4]*Forschungszentrum Jülich GmbH, ER-C and PGI, Jülich, Germany*
[5]*Forschungszentrum Jülich GmbH, JCNS-1 and ICS-1, Jülich, Germany*
[6]*European Spallation Source ERIC, Lund, Sweden*
[7]*Faculty of Physics and Center for Nanointegration Duisburg-Essen (CENIDE), University of Duisburg*
[8]*Paul Scherrer Institut, Swiss Light Source, Villigen, Switzerland*
[*]*a.feoktystov@fz-juelich.de*

Iron oxide nanoparticles are presently considered as promising objects for various medical applications including targeted drug delivery and magnetic hyperthermia. The nanoparticle solution in water has to posses large enough saturation magnetization to react on external magnetic field. However, there remains several unsolved questions regarding the effect of size onto nanoparticle overall magnetic behavior. One aspect is the reduction of magnetization as compared to bulk samples. A detailed understanding of the underlying mechanisms of this reduction will improve the particle performance in the applications.

There are several proposed models for the spatial distribution of the magnetization, which include the presence of a magnetic core-shell structure, spin disorder around defects and a reduced magnetization in the core due to reversed moments and frustration. In this work we combine neutron and synchrotron X-ray scattering techniques with magnetometry, transmission electron microscopy (TEM), elemental analysis and Mössbauer spectroscopy to study nanoparticles of various sizes and to obtain as complete as possible picture of their properties [1]. We find that the nanoparticles possess a macroscopically reduced saturation magnetization, mostly due to the presence of antiphase boundaries (APBs) as observed with high-resolution TEM (HRTEM) and X-ray scattering [2] and to a lesser extent due to a small magnetically depleted surface layer and cation vacancies.

References

[1] T. Köhler, A. Feoktystov, O. Petracic, E. Kentzinger, et al. *Nanoscale* 13 (2021) 6965.

[2] T. Köhler, A. Feoktystov, O. Petracic, N. Nandakumaran, et al. *J Appl Crystallogr* 54 (2021) 1719.

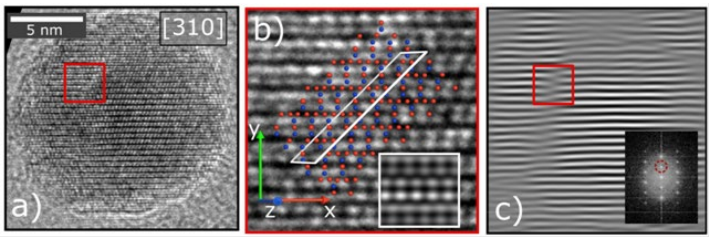

Figure 1. (a) HRTEM micrograph of an isolated nanoparticle viewed along [310]. A region with an APB is marked with the red square. (b) Marked region of (a) with a schematic of the crystal structure, the atom positions were verified by multislice TEM image simulations (inset). The lattice plane along which the translation occurs is indicated with the white rectangle. Red and blue dots represent iron atoms in octahedral and tetrahedral coordination, respectively. (c) The micrograph depicted in (a) after masking the 220 Bragg reflection (red circle in the inset) in the fast Fourier transform (FFT) and calculating the inverse FFT (IFFT). Now the lattice translation becomes clearly visible.

Steering the modes of deformation of soft magnetoelastic actuators by internal structuring

L. Fischer, A. M. Menzel

Institut für Physik, Otto-von-Guericke-Universität Magdeburg, Universitätsplatz 2, 39106 Magdeburg, Germany

Overview

Magnetic gels and elastomers are well known for their magnetoelastic effect. That is, their mechanical properties such as stiffness or dissipative behavior can be tuned from outside by external magnetic fields [1]. Yet and besides, they are also promising candidates to realize soft actuators. To this end, their magnetostrictive properties are exploited [2, 3]. Induced by homogeneous external magnetic fields, this allows for induced changes in shape also for microscopic objects in a contactless way.

Motivation

The considered materials consist of magnetizable particles of micrometer to submillimeter size embedded in a soft elastic polymeric matrix. The latter is sufficiently soft so that it is notably deformed when the particles are magnetized and exert resulting forces. Accordingly, induced magnetic interactions between the particles lead to overall deformation.

As a consequence, the discrete arrangement of the particles is directly related to the type of deformation emerging for the whole sample under consideration. It is our goal to relate these two scales of microscopic particles and overall macroscopic deformation. In other words, our ambition is to calculate explicitly from the discrete arrangement of the microscopic particulate inclusions the overall deformation of the whole system. This endeavor requires to include the system boundaries into our considerations. The displacement of these boundaries represents the induced overall deformation as viewed from outside.

Theoretical description

To be able to determine the overall deformation from the induced magnetic forces be-tween the discrete magnetized particles, we proceed by analytical calculations. These are performed in the framework of linear elasticity for isotropic, homogeneous, compressible or incompressible materials. Taking into account the boundaries of the sys-tem in a three-dimensional situation is challenging. Therefore, we consider a geometry as simple as possible and turn to objects of spherical shape.

For this case, an analytical expression for the corresponding Green's function is avail-able [4, 5]. That is, from the magnetic force centers, which we assume as point-like, we can calculate the mechanical displacements throughout the system and thus also on the surface of the sphere. The outward surface displacements determine the overall changes in shape. We expand the outward surface displacement field into spherical harmonics, which identify the different normal modes of deformation.

The influence of many force centers given by the many magnetized particles in the linearly elastic regime is simply superimposed. This is achieved by evaluating our analytical expressions using computational means.

Results

In effect, we now can calculate from the discrete arrangements of many particles inside our soft elastic composite system the resulting changes in overall macroscopic shape including the full

range of elastic degrees of freedom. We had demonstrated corresponding modes of deformation for isotropic and for regular lattice arrangements [5, 6], as well as for twisted particle configurations [7, 8]. The latter leads to torsional actuation, which recently has been realized in experiments [9].

Conclusions

In summary, we link microscopic properties, specifically the discrete arrangement of magnetizable particle in soft magnetic gels and elastomers, to the overall macroscopic deformation of the whole system. We demonstrate that peculiar overall modes of deformation can be obtained and pronounced by realizing specific microscopic particle con-figurations. With the advent and rapid evolution of new techniques of material synthesis, such as 3D printing, fabricating such systems in reality seems in reach. In this way, tailored soft magnetoelastic actuators selected for a specific practical purpose can be generated in the future.

Acknowledgments

We thank the German Research Foundation (DFG) for support through the Heisenberg Grant no. ME 3571/4-1/4-2.

References

[1] S. Odenbach, Arch. Appl. Mech. 86, 269 (2016).
[2] A. M. Menzel, Phys. Rep. 554, 1 (2015).
[3] A. M. Menzel, H. Lowen,¨ Phys. Sci. Rev. 7, 1529 (2022).
[4] L. J. Walpole, Proc. R. Soc. London A 458, 705 (2002).
[5] L. Fischer, A. M. Menzel, J. Chem. Phys. 151, 114906 (2019).
[6] L. Fischer, A. M. Menzel, Smart Mater. Struct. 30, 014003 (2021).
[7] L. Fischer, A. M. Menzel, Phys. Rev. Research 2, 023383 (2020).
[8] A. M. Menzel, J. Chem. Phys. 154, 204902 (2021).
[9] M. T. Lopez-Lopez, Presentation at the CECAM Flagship Workshop "Emerging colloidal dynamics away from equilibrium. Chiral active systems." (Lausanne, Switzerland, 2023).
[10] L. Fischer, A. M. Menzel, to be submitted (2023).
[11] D. Günther, D. Y. Borin, S. Günther and S. Odenbach, Smart Mater. Struct. 21, 015005 (2012)

A unified modeling framework for soft and hard magneto-active polymers at the macroscale level

Philipp Gebhart, Thomas Wallmersperger

Institute of Solid Mechanics, Technische Universität Dresden, 01062 Dresden, Germany

In recent years there has been an increasing interest in the theoretical and experimental study of field responsive, functional composite materials. Magneto-active polymers (MAPs) are a special class of field responsive solids that comprise of a polymeric matrix with dispersed micro-sized magnetizable particles. Based on the magnetic properties of the underlying ferromagnetic filler particles, MAP composites can be classified into two categories: (i) soft and (ii) hard MAPs.
Soft MAPs comprising magnetically soft particles, e.g. carbonyl iron, exhibit negligible hysteresis loss and demagnetize completely after the removal of the external magnetic field which in consequence leads to reversible deformation mechanisms. In contrast, NdFeB particle-filled hard MAPs exhibit distinct nonlinear, dissipative material behavior, such as the characteristic magnetic and ”butterfly” field-induced strain hysteresis. In the present work, we present a comprehensive variational-based modeling framework for hard MAPs including the response of the soft MAPs as a limiting case. We outline ingredients of the constitutive theory based on the framework of generalized standard materials, that necessitates suitable definitions of (i) the total energy density function and (ii) the dissipation potential.
Key idea of the constitutive approach is an additive split of the material part of the total energy density function into three contributions associated with (i) an elastic ground-stress, (ii) the magnetization and (iii) a magnetically induced mechanical stress, respectively [1, 2]. We propose suitable constitutive functions in an energy-based setting that allow to accurately capture the highly non-linear material behavior of soft and hard MAPs with stochastic microstructures. The performance of the developed variational-based modeling framework is demonstrated by solving some application-oriented boundary value problems. The main emphasis of the numerical studies lies on the investigation of the magnetostrictive effect of hard MAPs at the macroscale level as well as on the in depth analysis of pre-magnetized beam structures undergoing large deformations.

Acknowledgments

This research has been financially supported by the Deutsche Forschungsgemeinschaft in the framework of the Priority Programme SPP1681.

References

[1] P. Gebhart and T. Wallmersperger, A constitutive macroscale model for compressible magneto-active polymers based on computational homogenization data: Part I - Magnetic linear regime, IJSS, 236, 111294, 2022

[2] P. Gebhart and T. Wallmersperger, A constitutive macroscale model for compressible magneto-active polymers based on computational homogenization data: Part II - Magnetic non-linear regime, IJSS, 258, 111984, 2022

Macroscopic and microscopic properties of thermoplastic polyurethane magnetorheological elastomers

D. Kare Gowda, S. Odenbach

Chair of Magnetofluiddynamics, Measuring and Automation Technology, TU Dresden, 01069 Dresden, Germany

Introduction

Magnetorheological elastomers (MREs) are elastomer composites with embedded magnetic particles. Due to their rapid response to stimulation by an external magnetic field they are classified as smart materials. The MREs made of thermoplastic elastomers can be stimulated by both temperature and magnetic field. In recent times, thermoplastic polyurethane magnetorheological elastomers (TPU-MREs) have attracted considerable interest among researchers due to its multi stimulated compliance in addition to superior mechanical properties, ease of preparation and wide range of applicability [1,2]. The change in modulus of an MRE in response to an applied external magnetic field provides information on the sensitivity of the MRE. The investigation of particle microstructure provides further information on the reason behind the changes in mechanical properties. X-ray micro tomography has been proved to be a reliable tool for microstructural investigation [3,4]. In this work we present the temperature and magnetic field dependent changes in mechanical and microstructural properties of TPU-MRE.

Materials and methods

TPU-MRE samples were prepared from a two component TPU system. PU 450 and PH 330 from Elantas were mixed with plasticizer Dimethyl Phthalate from Sigma-Aldrich and Höganas ASC 200 iron particles of size 50 to 80 µm. The composition of the investigated samples contained 40, 50 and 60 wt.% of iron particles within the TPU matrix material. The TPU components are weighed based on the parts by weight calculation, and the plasticizer and iron particles as percentage weight. The details of the method of calculation and preparation process can be found in our previous article [5].

Isotropic cylindrical rod-shaped samples were tested for mechanical properties based on the method proposed in Borin et.al. [6]. Quasi-static tensile and torsion tests were conducted using a modified HAKE MARS III rheometer. All the tests were conducted at three different temperatures with and without the presence of a magnetic field of 250 mT. As the quasi-static tensile and torsion tests were conducted within the linear elastic limit of the sample, the slopes of the corresponding stress-strain curves provide the values of the Young's modulus (E) and the shear modulus (G). Table 1 shows the sequence in which the samples were tested. The relative difference between the modulus with and without magnetic field gives the magnetorheological effect (MR effect).

Table 1. Sequence of quasistatic tensile (E) and torsion (G) tests on the sample.

Temp.	23 °C		40 °C		60 °C	
Test	E	G	E	G	E	G
0 mT	1	3	5	7	9	11
250 mT	2	4	6	8	10	12

Microstructural investigations using X-ray microcomputed tomography was done on the sample with 40 wt.% of iron particles. The samples were observed for microstructural changes at 23 °C and 60 °C without and with a magnetic field of 250 mT. The microstructural arrangement of particles was investigated using previously established direction dependent pair correlation function (PCF) and the particle motion was studied using particle tracking technique [4]. The influence of different stimulating conditions was studied in both macro- and microscopic scale.

Results and Discussion

From figure 1, the results indicate that the MR effect calculated from both the Young's and the shear modulus of the TPU-MRE sample increase with the increase in temperature. With the increase in temperature, the bonding force between the soft and hard segments reduces, leading to higher freedom of movement for soft segments. This results in the decrease in the modulus with the increase in temperature and hence increase in MR effect. It can be clearly observed that the magnitude of MR effect is slightly higher in tensile tests than in torsion tests. This is due to the difference in direction of strain with respect to the direction of the magnetic field. The inter particle force of attraction is higher along the magnetic field direction. Therefore, the resistance to deformation experienced by the sample in presence of magnetic field is higher in tensile tests than in torsion tests and resulting in higher MR effect.

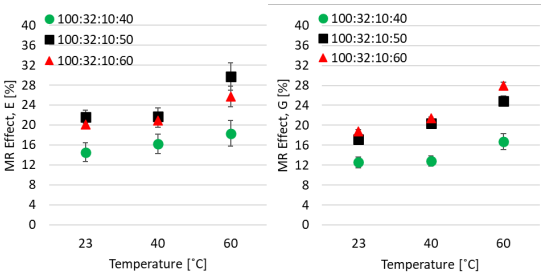

Figure 1. The calculated MR effect of the Young's modulus (E) (left) and shear modulus(G) (right).

Microstructural investigation preliminarily revile that the particles are homogenously distributed in the sample. Figure 2. shows the distribution along the length of the sample.

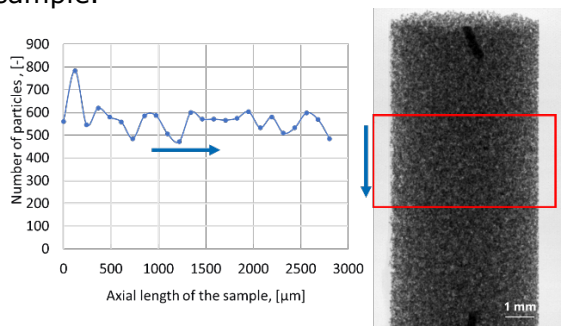

Figure 2. Particle distribution along axile direction.

Acknowledgments

The authors would like to express their thanks to the Deutsche Forschungsgemeinschaft (DFG) for financial support within the SPP2100 research program (OD 18/28-1).

References

[1] Bastola, A. K., Paudel, M., Li, L., and Li, W., "Recent progress of magnetorheological elastomers: a review," *Smart Materials and Structures*, Vol. 29, No. 12, 1 Jan. 2020, p. 123002. doi: 10.1088/1361-665X/abbc77.

[2] Zhang, G., Zhang, Z., Sun, M., Yu, Y., Wang, J., et al., "The Influence of the Temperature on the Dynamic Behaviors of Magnetorheological Gel," *Advanced Engineering Materials*, 1 Jan. 2022, p. 2101680. doi: 10.1002/adem.202101680.

[3] Gundermann, T., Cremer, P., Löwen, H., Menzel, A. M., and Odenbach, S., "Statistical analysis of magnetically soft particles in magnetorheological elastomers," *Smart Materials and Structures*, Vol. 26, No. 4, 1 Jan. 2017, p. 45012. doi: 10.1088/1361-665X/aa5f96.

[4] Schümann, M., Borin, D. Y., Morich, J., and Odenbach, S., "Reversible and non-reversible motion of NdFeB-particles in magnetorheological elastomers," *Journal of Intelligent Material Systems and Structures*, Vol. 32, No. 1, 1 Jan. 2021, pp. 3–15. doi: 10.1177/1045389X20949703.

[5] Kare Gowda, D., and Odenbach, S., "Investigation of quasistatic and dynamic mechanical properties of thermoplastic polyurethane magnetorheological elastomers," *Journal of Magnetism and Magnetic Materials*, Vol. 579, 1 Jan. 2023, p. 170856. doi: 10.1016/j.jmmm.2023.170856.

[6] Borin, D., Kolsch, N., Stepanov, G., and Odenbach, S., "On the oscillating shear rheometry of magnetorheological elastomers," *Rheologica Acta*, Vol. 57, No. 3, 1 Jan. 2018, pp. 217–227. doi: 10.1007/s00397-018-1071-2.

Neural network-based multiscale modeling of finite strain magneto-elasticity with relaxed convexity criteria

K.A. Kalina[1,2], P. Gebhart[1], J. Brummund[1], L. Linden[1], W. Sun[2], M. Kästner[1,3]

[1] *Institute of Solid Mechanics, TU Dresden, Dresden, 01062, Germany*
[2] *Department of Civil Engineering and Engineering Mechanics, Columbia University, New York, NY 10027, USA*
[3] *Center for Computational Materials Science, TU Dresden, Dresden, 01062, Germany*

We present a framework for the multiscale modeling of finite strain magneto-elasticity which is based on physics-augmented neural networks (NNs). By using a set of problem specific invariants as input, an energy functional as the output and by adding several non-trainable expressions to the overall total energy density functional, the model fulfills multiple physical principles by construction, e.g., thermodynamic consistency, material symmetry or a stress-free and non-magnetized unloaded configuration.

Three NN-based models with different levels of rigor regarding an extended polyconvexity condition and the growth condition of the magneto-elastic potential are presented. First, polyconvexity, which is a global concept, is enforced via input convex neural networks (ICNNs), i.e., by construction. Afterwards, we formulate a relaxed local version of the polyconvexity and fulfill it in a weak sense by adding a tailored loss term. Furthermore, as an alternative, a loss term to enforce the weaker requirement of strong ellipticity locally is proposed, which can be favorable to obtain a better trade-o between compatibility with data and physical constraints.

Databases for training of the models are generated via computational homogenization for both compressible and quasi-incompressible magneto-active polymers (MAPs). Thereby, to reduce the computational cost, 2D statistical volume elements and an invariant-based sampling technique for the pre-selection of relevant states are used. All models are calibrated by using the database, whereby interpolation and extrapolation are considered separately. Furthermore, the performance of the NN models is compared to a conventional model from the literature. The numerical study suggests that the proposed physics-augmented NN approach is advantageous over the conventional model for MAPs. Thereby, the two more flexible NN models in combination with the weakly enforced local polyconvexity lead to good results, whereas the model based only on ICNNs has proven to be too restrictive.

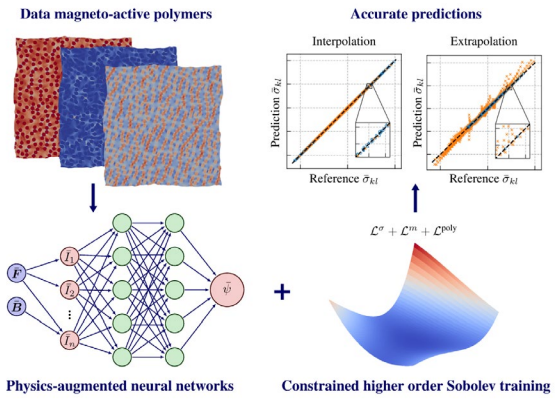

Figure 1. Workflow for data-driven multiscale modeling of finite strain magneto-elasticity

Acknowledgments

All presented computations were performed on a PC-Cluster at the Center for Information Services and High Performance Computing (ZIH) at TU Dresden. The authors thus thank the ZIH for generous allocations of computer time. This work was supported by a DAAD Fellowship to Karl A. Kalina.

References

[1] KA Kalina, P Gebhart, J Brummund, L Linden, WC Sun, M Kästner: Neural network-based multiscale modeling of finite strain magneto-elasticity with relaxed convexity criteria. arXiv preprint arXiv:2308.16311, 2023.

Extended treatment of particle magnetisation in molecular dynamics simulations

Kantorovich S.S.[1], Kuznetsov A.[1], Mostarac D.[1], Rosenberg M.[1], Helbig S.[1], Suess D.[1]

[1] *University of Vienna, Vienna, Austria*

Following experimental advances in the early 2000s, anisotropic and anisometric magnetic nanoparticles have become a promising subfield of magnetic soft matter [1,2]. It has been shown that even small alternations in particle shape strongly affect the overall microscopic properties of such particle suspensions [3]. This particular feature makes them

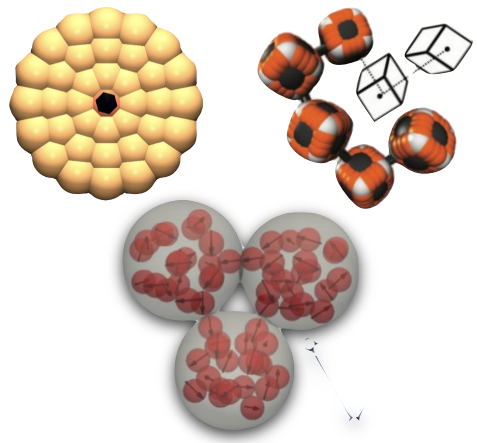

Figure 1. Magnetic platelets with extended dipoles; magnetic filaments; magnetic multicore particles.

appealing candidates for applications with tailored requirements [4]. What is not yet clear, albeit being of primary interest, it is how the dynamics of the systems of anisotropic and anisometric particles is affected by their intrinsic features.

Here, we present an extensive study on how to correctly merge intrinsic magnetisation processes of nanoparticles with their spatial motion and structural transitions in molecular dynamics simulations. We put forward three different approaches based on the egg-model [5], on a so-called hot Stoner-Wohlfarth paradigm [6] and on the extended dipoles [7] to allow for particle magnetic nature. We apply those models to investigate static and dynamic susceptibilities of the systems as well as the cluster formation dynamics.

In particular, we focus on magnetic multicore spherical particles, magnetic filaments and platelets, as shown in the Figure .

References

[1] S. Sacanna and D. J. Pine, Current Opinion in Colloid and Interface Science, 2011, 16, 96–105.

[2] L. Rossi, S. Sacanna, W. T. M. Irvine, P. M. Chaikin, D. J. Pine and A. P. Philipse, Soft Matter, 2011, 7, 4139–4142.

[3] J. G. Donaldson, E. S. Pyanzina and S. S. Kantorovich, ACS Nano, 2017, 11, 8153–8166.

[4] P. Tierno, Phys. Chem. Chem. Phys., 2014, 16, 23515–23528.

[5] V. I. Stepanov, M. I. Shliomis, Bulletin of the Russian Academy of Sciences: Physics, 1991, 55, 1-8.

[6] M.A. Chuev, J. Hesse, J. Phys.: Condens. Matter, 2007, 19**,** 506201(18p).

[7] G. Steinbach, D. Nissen, M. Albrecht, E. Novak, P. A. Sánchez, S. S. Kantorovich S et al. Soft Matter, 2016, 12, 2737-2743.

Magnetic alignment and particle mobility of anisotropic hematite nanoparticles

J. Kopp[1], J. Landers[1], B. Rhein[2], G. Richwien[2], A. Schmidt[2], and H. Wende[1]

[1]*Faculty of Physics and Center for Nanointegration Duisburg-Essen (CENIDE), University of Duisburg-Essen*
[2]*Institute for Physical Chemistry, University of Cologne*

Abstract

Nowadays, ferrofluids and magnetic hybrid materials play an important role in many technical applications, allowing tunable reaction to external stimuli depending on the magnetic properties of the embedded nanoparticles as well as the particle mobility, defined by the particles' size, shape, and nanoscale surrounding. Therefore, we here present a study on the magnetic nanoparticle alignment in ferrofluids being exposed to magnetic fields, as well as on the shape-dependent anisotropic diffusion. This approach later on is planned to be applied to functional hybrid materials of more complex nanostructure. For that purpose, we performed magnetometry and Mössbauer spectroscopy experiments of about 1 wt% of hematite nanoparticles of different aspect ratio ranging from ~1 (approximately spherical) to 5.13 (spindle-shaped) in 70 wt% glycerol-water solution. Scanning transmission electron microscopy (STEM) images are shown in fig 1 and 2, respectively. Based on previous experiments on the in-field alignment behavior of oxide nanoparticles in ferrofluids, Mössbauer spectroscopy experiments were conducted in different

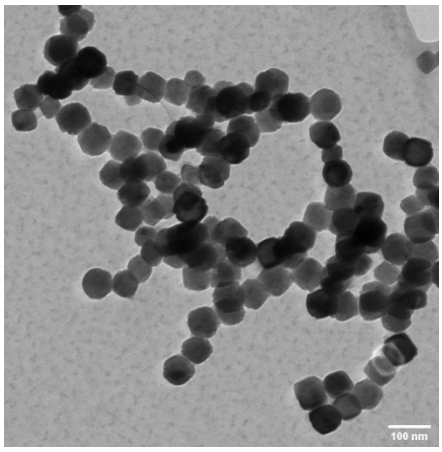

Figure 2. STEM image of hematite nanoparticles with aspect ratio of about 1

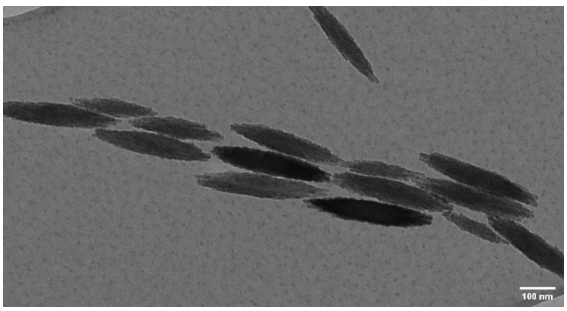

Figure 1. STEM image of hematite nanospindles with aspect ratio 5.13

experimental geometries, corresponding to perpendicular and parallel orientation of the magnetic field relative to the γ-ray incidence (probing) direction [1]. As Mössbauer spectroscopy utilizes the linear optical Doppler effect, by doing so we aim for information on particle diffusion coefficients along probing direction, yielding anisotropic diffusion coefficients for the nanospindles in case of complete particle alignment in sufficiently high magnetic fields. Information on the magnetic alignment of the nanospindles can be extracted by analyzing the relative line intensity ratio A_{23} of lines 2 and 3, as shown in Fig. 3, where A_{23} = 4/3 corresponds to a complete magnetic alignment along field direction, whereas A_{23} = 4 translates to a complete spin alignment perpendicular to the probing direction. As we can see in Fig. 3, we achieve almost complete alignment along field direction at about 70 mT. At the same time, linewidths extracted from Mössbauer spectroscopy were compared for different probing directions as well as for different particle shapes, to indicate the presence of anisotropic diffusion of the elongated particles when being aligned via magnetic fields. In fact, the first results for the elongated particles showed a weakening in the case of perpendicular geometry and a reinforcement of the particle diffusion for the parallel geometry.

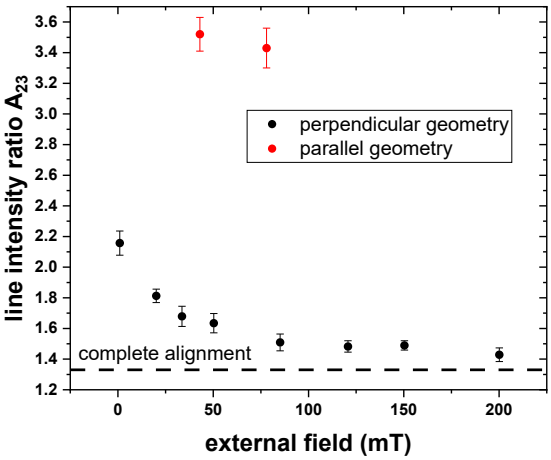

Figure 3. Line intensity ratio A_{23} as a function of the external magnetic field of the sample with an aspect ratio of 5.13 in parallel and perpendicular geometry.

Outlook

The main objective of this work is to study the orientation process of hematite nanospindles with different aspect ratios in magnetic fields as well as the influence of the field on the particle motion. In the next step, we want to extend our approach from ferrofluids to liquid crystalline systems and study in detail the particle dynamics in ferronematic phases to gain more insight on anisotropic diffusion. In this context, first attempts to stabilize barium ferrite nanoplatelets in 5CB have already been performed.

Acknowledgments

We gratefully acknowledge funding by the DFG through LA5175/1-1.

References

[1] J. Landers, S. Salamon, H. Remmer, F. Ludwig, and H. Wende, *In-Field Orientation and Dynamics of Ferrofluids Studied by Mössbauer Spectroscopy,* ACS Appl. Mater. Interfaces, 11, 3160-3168 (2019)

Magneto-elastomeric nanocomposites based on polymer-coated nanoparticles

M. Kruteva

Jülich Centre for Neutron Science, Forschungszentrum Jülich GmbH, 52428 Jülich

Functional materials consisted of polymer-coated nanoparticles tend to self-assemble into complex structures and widely used for biomedical and industrial applications. The precise control of the nanoparticle assembly is crucial for obtaining magneto-elastomeric nanocomposites with desirable properties. For that, internal parameters of a system are tuned, such as *e.g.* the polymer shell size, constituting materials, solvent. Additionally, nanoparticle assembly can be impacted by external influences: shearing, magnetic fields (applied to magnetic-core nanoparticles), temperature, which leads to the formation of highly ordered structures.

In framework of the SPP 1681 we developed a synthetic procedure to obtain highly monodisperse nanoparticles consisting of a superparamagnetic iron oxide core (SPION) embedded in a polymeric shell [1,2]. Using a combination of scattering techniques with TEM we showed that particle agglomeration is largely absent. Our scattering experiments in solution or in the solvent free state in the presence of a magnetic field demonstrated (i) chain-like ordering of the nanoparticles along the direction of the magnetic field and (ii) a pronounced magnetic scattering observed by small angle neutron scattering (SANS).

Recently it has been demonstrated that controlled synthesis of SPIONs applying a thermal pretreatment of the iron oxide precursor is possible [3]. We find that each solvent provides access to a certain temperature range, within which the variation of temperature, heating rate, or precursor concentration allows us to reproducibly control the nanoparticle size Further, grafting the SPIONs with polymer using ligand exchange was performed. For that polystyrene (PS) and polyisoprene (PI) was used. Shearing and magnetic external fields are powerful instruments for structure ordering and orientation, which enable phase transitions and the adjustment of lattice parameters. Accordingly, polymer grafted SPIONs form FCC crystal phases under shearing, which in combination with a permanent magnetic field causes reorientation processes of the nanoparticles. In particular, the influence of a permanent magnetic field during a long-time exposure causes well-defined disorder-BCC-FCC phase transitions [4].

The dynamics and conformation of grafted polymer is governed by the assembly of nanoparticles in melt state [5]. This assembly in turn is significantly dictated by the polymer properties. We studied the rheological response of PI grafted nanoparticles with two different molecular weights. We show that for unentangled grafted PI, the geometrical confinements from the assembly of nanoparticle solely governs the apparent rheology plateau. On the other hand, for weakly entangled polyisoprene, a combination of geometrical confinements and topological entanglements from polymer chains gives rise to a prominent plateau in the frequency sweep. We showed that a correct analysis of small angle X-ray scattering (SAXS) data is crucial to these results and the famously used hard sphere model is not applicable to these systems. Using a combination of SAXS and rheology, we were able to interpret the dynamics and conformation of grafted polymer chains in context of the assembly of the nanoparticles.

References

[1] R. Koll *et al.*, Nanoscale (2019) 11 (9), 3905–3915
[2] A. Feld *et al*., ACS Nano (2017) 11 (4), 3767–3775
[3] V. Fokina et al., J. Phys. Chem. C (2022) 126 (50) 21356–21367
[4] V. Fokina *in preparation*
[5] A. Sharma et al. Macromolecules (2023) 56 (13), 4952-4965

Magnetic field dependence of the dynamics of BaHF nanoplatelet suspensions

M. Küster[1], H. Nádasi[2], A. Eremin[2], F. Ludwig[1]

[1] *Institut für Elektrische Messtechnik und Grundlagen der Elektrotechnik und LENA, TU Braunschweig, Braunschweig, Germany*
[2] *Institut für Physik, ANP, Otto-von-Guericke-Universität Magdeburg, Magdeburg, Germany*

Introduction

Tuning the macroscopic properties of ferrofluid suspensions enables a multitude of application areas. In order to do so, it is of uttermost importance to understand the microstructure, reflecting the nanoscale characteristics of the suspensions. Following the theoretical prediction of a fluid ferromagnet more than 50 years ago, it has only recently been shown that even in suspensions of ferrimagnetic bariumhexaferrite (BaHF) nanoplatelets in isotropic n-butanol colloidal nematic phases can form [1-3]. In order to understand the self-assembly mechanism stabilizing the order, an analysis of the energies involved is necessary.

Studying the dynamic magnetization spectra of BaHF suspensions in 1-butanol, we found that multiple relaxation modes can appear in the complex susceptibility spectrum [4]. Given the fact that these modes cannot be described by a single Debye-type mechanism, we attribute them to a superposition of single-particle relaxation at high frequencies and low-frequency relaxation modes, which we assign to self-assembled structures [4,5].

In this contribution we show how both the relaxation of single particles and that of the low-frequency collective modes change depending on external alternating (AC) and static bias (DC) fields, either parallel or perpendicular to the excitation direction.

Experiment

Scandium-doped barium hexaferrite (BaHF) nanoplatelets with DBSA surfactant [1] were suspended in isotropic 1-butanol with concentrations between 7.5 mg/mL and 304 mg/mL. The magnetic moments of these nanoplatelets are directed perpendicularly to their basal planes. The sample with the highest BaHF nanoplatelet concentration (304 mg/mL) exhibits nematic order. The sample studied here has a fixed mass ratio of particles to DBSA of 87:13, which was found to be optimum considering the interplay of magnetic and electrostatic interactions [5], and a platelet concentration of 75 mg/mL. The dynamics of the BaHF platelets is studied using AC susceptometry in a frequency range from 0.1 Hz – 2.2kHz using a fluxgate-based setup [6]. The applied AC magnetic field amplitude was varied up to 5 mT, additionally DC fields were superimposed with strengths up to 1 mT, being directed either parallel or perpendicular to the AC field.

Results

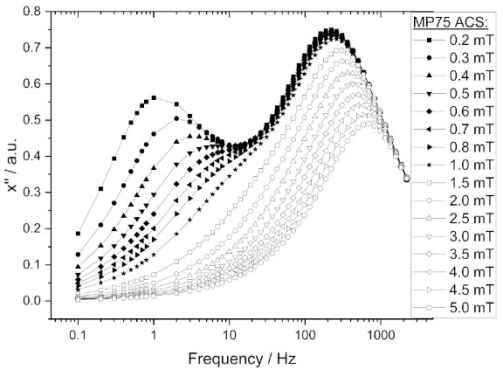

Figure 1. ACS spectra of MP75, measured for different AC field amplitudes ranging from 0.2 mT to 5 mT.

Fig. 1 depicts the ACS spectra measured for different AC field amplitudes. Two relaxation modes are clearly discernable: the mode at high frequencies is attributed to the relaxation of single platelets while the middle-frequency (MF) mode is caused by self-assembled structures [4,5]. The peak frequency of both modes shifts with increasing AC field amplitude towards higher frequencies. The fit of the

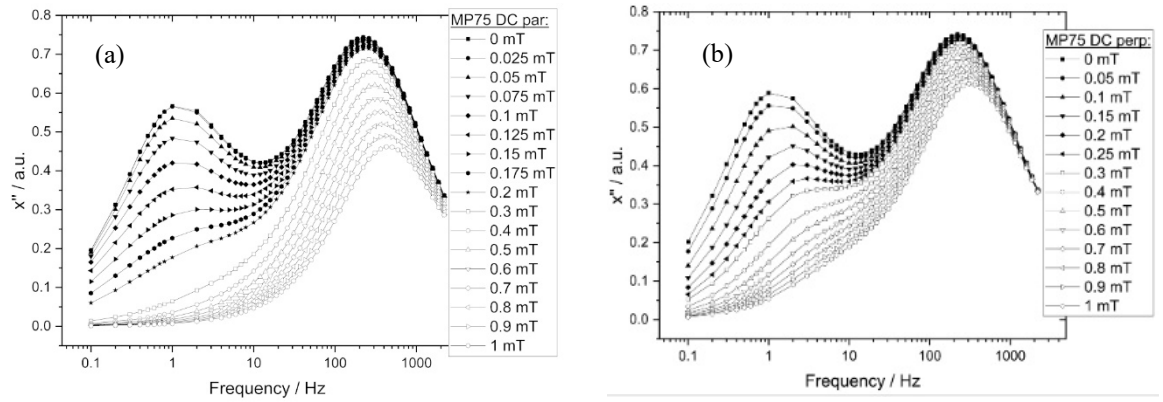

Figure 2. ACS spectrum (0.2 mT) with superimposed DC offset fields, (a) parallel and (b) perpendicular to AC field.

field dependence of the characteristic frequency of the HF mode with the Fokker-Planck-based phenomenological equation by Yoshida and Enpuku [7] works reasonably well but provides a too large value of the platelet's magnetic moment. Analyzing the data with the equation derived by Rusanov et al. [8] for interacting particles results in a better fit, which additionally provides the effective Langevin susceptibility of interacting nanoparticles.

As Figs. 2 (a) and b) show the shift and suppression of the MF peak significantly differ for additionally applied DC fields parallel and perpendicular to the AC field. The fact that the shift and suppression is larger for an applied parallel DC field is in qualitative agreement with theory [9], which however considers non-interacting nanoparticles.

Conclusion and outlook

Both the relaxation time of single platelets and that of collective modes show a pronounced dependence on the applied AC and DC magnetic field. For medium platelet concentrations, dipolar interactions cannot be neglected; here the equation derived by Rusanov et al. [8] well explains the dependence of the Brownian relaxation time of single platelets on AC magnetic field. The strong shift and suppression of the mode related to self-assembled structures by a superimposed DC magnetic field, directed either parallel or perpendicular to the AC field, is an indication of the considerably higher and magnetic-field dependent magnetic moment of these structures

Acknowledgement

The research was funded by the DFG via projects LU 800/7-1 and NA 1668/1-1. The authors acknowledge P. H. Boštjančič from the Jožef Stefan Institute Ljubljana for providing the BaHF platelet suspensions.

References

[1] A. Mertelj et al., *Nature* 504, 237-241 (2013).
[2] N. Sebastián et al., *Soft Matter* 14, 7180-7189 (2018).
[3] M. Shuai et al., *Nat. Commun.* 7, 10394 (2016).
[4] M. Küster et al., *J. Mol. Liq.* 360, 119484 (2022).
[5] H. Nádasi et al., *J. Mol. Liq.* 382, 121900 (2023).
[6] J. Dieckhoff et al., *Appl. Phys. Lett.* 99, 112501 (2011).
[7] T. Yoshida and K. Enpuku, *Jpn. J. Appl. Phys.* 48, 127002 (2009).
[8] M. S. Rusanov et al., *Physical Review E* 104, 044604 (2021).
[9] M. A. Martsenyuk et al., *Sov. Phys. JETP* 38, 3507 (1974).

Laser-tuning of magnetic and catalytic properties in spinel-based ferrofluids

J. Landers[1], S. Zerebecki[2], S. Salamon[1], D. Krenz[2], A. Rabe[1], S. Reichenberger[2], S. Barcikowski[2], H. Wende[1]

[1] *Faculty of Physics and Center for Nanointegration Duisburg-Essen (CENIDE), University of Duisburg-Essen*
[2] *Technical Chemistry I and Center for Nanointegration Duisburg-Essen (CENIDE), University of Duisburg-Essen*

Ferrimagnetic spinel-type nanoparticles are widely used in technical as well as medical applications due to their stability, high magnetization and tunable coercivity. An essential material parameter defining the cation distribution is the so-called inversion parameter "x". It describes the distribution of the different metal ions on octahedral (B-) and tetrahedral (A-) sublattice positions, specified e.g. by: $(M^{2+}_{1-x}Fe^{3+}_{x})_A(M^{2+}_{x}Fe^{3+}_{2-x})_B O_4$.
Evidently, the distribution of different ion species on the A- and B-sublattice has a dramatic influence on the magnetic properties of the spinel, most directly on the saturation magnetization M_S. A simple calculation shows that e.g. in cobalt ferrite M_S is expected to increase by about 40% when going from the well-ordered inverse spinel structure to random ion placement.
This has been previously demonstrated in spinel bulk samples or powders by tuning the inversion parameter via heat treatment followed by cooldown at different cooling rates to obtain different degrees of order in ion placement [1], as illustrated in figure 1. However, the excessive initial heating required for this method is

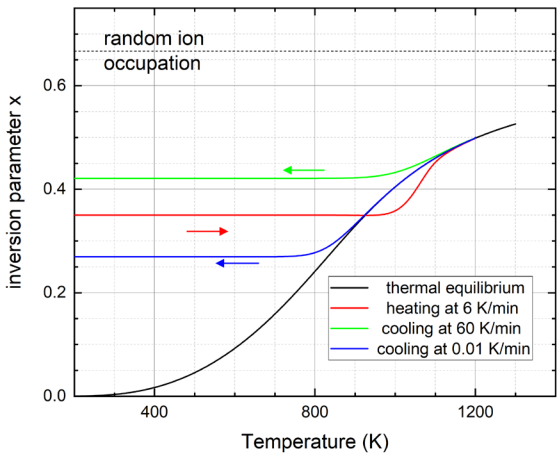

Figure 1. Exemplary calculation of the inversion parameter x in an inverse spinel upon annealing to 1200 K for different cooling rates, x_0 = 0.35.

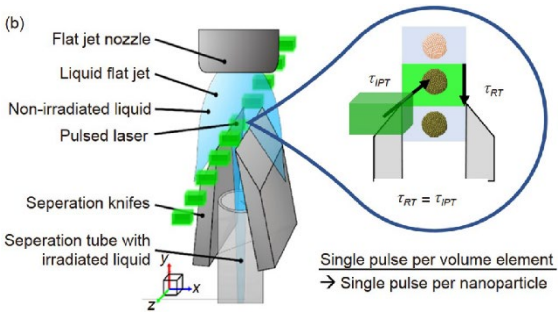

Figure 2. Scheme of the flat-jet setup used for s-PUDEL under continuous flow conditions. [2]

impractical for small nanoparticles due to potential sintering, which can cause considerable particle growth and morphology changes. Here, an option has been introduced recently, utilizing single nanosecond laser pulses for the controlled heating (and diffusion enhancement) of the spinel nanoparticles in a fluid stream (s-PUDEL [2]). A schematic overview of the setup used for this approach is shown in figure 2. During the laser processing, the nanoparticles experience elevated temperatures for only a few tens of nanoseconds such that atomic diffusion and modification of the inversion parameter can take place in a confined volume and controlled time frame, respectively. Due to the rapid heat transfer from the laser-heated particles into the surrounding fluid (cooling rates of about 10^9 K/s), the heat-induced cation distribution is quenched and conserved within the laser-processed nanoparticles.
Within this study the method is demonstrated at the example of three different types of cobalt ferrite nanoparticles obtained from different synthesis techniques with different initial levels of disorder regarding the cation distribution. Precise measurements of the spinel inversion parameter were performed via Mössbauer spectroscopy in a magnetic field of 5 T following exposure of the particles to different laser dosages.

As visible in figure 3, increasing laser dosages led to ion redistribution, with the different particle types approaching the state of thermal equilibrium from different directions. The latter lies between the inverse spinel structure preferred for cobalt ferrite and a value of 2/3, which represents random ion placement. Following this approach, we have demonstrated the ability to tune the inversion parameter (and thereby the magnetization) of spinel nanoparticles with single laser pulses while maintaining the initial particle size and morphology. Finally, a linear correlation between the determined inversion parameter and the catalytic activity of the laser-processed particles in the conversion of cinnamyl alcohol could be shown in this study.

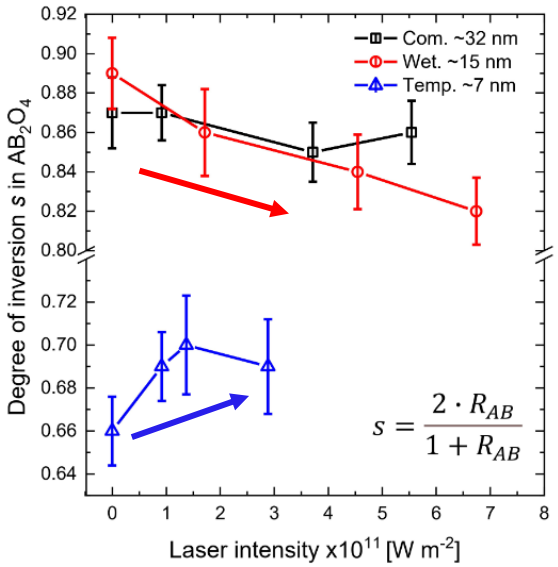

Figure 3. Laser-dose dependent change in inversion parameter x of three types/sizes of $CoFe_2O_4$ nanoparticles approaching the high-temperature thermal equilibrium state. [3]

In an ongoing study, we now aim to generalize this structure-activity correlation towards a broader matrix of laser-processed ferrite spinel systems (MFe_2O_4 with M = Mn, Co, Ni, Zn, …), to clarify to what extent the magnetic performance of spinel nanoparticles can be enhanced by tuning the inversion parameter, e.g., to lower necessary particle concentrations in medical applications.

Acknowledgements

Financial support by the German Research Foundation (DFG) via the CRC/TRR 247 (Project-ID 388390466, sub-projects B2 and C5) is gratefully acknowledged.

References

[1] M. R. de Guire et al., "The cooling rate dependence of cation distributions in $CoFe_2O_4$", *J. Appl. Phys.* **65**, 3167-3172 (1989)

[2] S. Reichenberger, "Freezing crystallographic defects into nanoparticles: The development of pulsed laser defect engineering in liquid (PUDEL)", *Sci. China-Phys. Mech. Astron.* **65**, 274208 (2022)

[3] S. Zerebecki et al., "Engineering of Cation Occupancy of $CoFe_2O_4$ Oxidation Catalysts by Nanosecond, Single-Pulse Laser Excitation in Water", *ChemCatChem* **14**, e2021101785 (2022)

Magnetic removal of *Candida albicans* using salivary peptide-functionalized SPIONs

Stefan Lyer[1,4], Bernhard Friedrich[1], Michaela Dümig[2], Alexandru Sover[3], Marius-Andrei Boca[3], Eveline Schreiber[1], Julia Band[1], Christina Janko[1], Sven Krappmann[2], Rainer Tietze[1*] and Christoph Alexiou[1*]

1 *Department of Otorhinolaryngology, Head and Neck Surgery, Section of Experimental Oncology and Nanomedicine (SEON), Else Kröner-Fresenius-Stiftung Professorship, Universitätsklinikum Erlangen, Erlangen, Germany*
2 *Mikrobiologisches Institut – Klinische Mikrobiologie, Immunologie und Hygiene, Universitätsklinikum Erlangen, Friedrich-Alexander-Universität (FAU) Erlangen-Nürnberg, Erlangen, Germany.*
3 *Faculty of Engineering, Ansbach University of Applied Sciences, Ansbach, Germany*
4 *Department of Otorhinolaryngology, Head and Neck Surgery, Section of Experimental Oncology and Nanomedicine (SEON), Professorship for AI-Controlled Nanomaterials, Universitätsklinikum Erlangen, Erlangen, Germany*
**These authors contributed equally to this work.*

Introduction

Fungal infections are a frequently underestimated clinical picture associated with both severe local and systemic inflammatory reactions. These microorganisms are known to cause a variety of host reactions that can lead to hypersensitivity disorders, toxic reactions and sepsis. Such types of infectious diseases, called mycoses, are categorized according to their causative agent (e.g. candidiasis, cryptococcosis, and aspergillosis) and primarily affect immunocompromised individuals[1]. Factors such as viral pan- and endemics (HIV, SARS-CoV-2), an ageing society, increasing numbers of surgical procedures have increased the number of patients, who are prone to opportunistic infections[2]. Especially in the case of candidiasis, the rather long-time spans until positive detection vary greatly. The most dominant and clinically most relevant yeast species to cause bloodstream infections is *Candida albicans* by far[1-4] with a medium time to detection of around 85 h. These examples demonstrate how important finding possibilities to accelerate fungal blood infections are. During this time usually the patients receive broad band antibiotics that unfortunately do not help against fungal infections. In our study, we investigated previously developed, GP340-peptide-functionalized SPIONs[5] for their capacity to extract *C. albicans* from different media under static and flow conditions. This was accompanied by theoretical simulations. Moreover, we investigated the feasibility to regrow the extracted fungal cells on culture plates and checked relevant interactions of the functionalized nanoparticles with different host cells.

Results

Characterization of SPION-APTES-Pep

To further study the organic content of SPION-APTES-Pep, thermographimetric (TGA) analysis revealed a first weight loss below 200°C, as it is known for other SPIONs. Further heating revealed a content of 12.3% peptide and linker and another 5.7% of the silane coating. This was confirmed by subsequent measuring the iron content of the probes with atomic adsorption spectroscopy (AES).

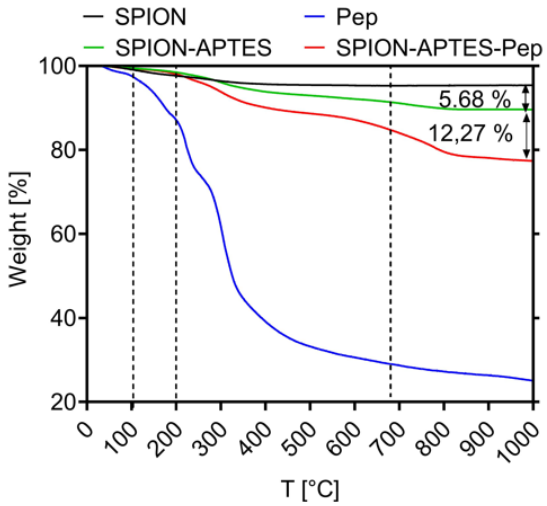

Figure 1. TGA curves of SPION, SPION-APTES, the pure peptide and SPION-APTES-Pep.

Storage stability of SPION-APTES-Pep

For any substance or nanoparticle being intended for the use in therapy or (*in vitro*)-diagnostic, storage stability is a critical factor. Here, an initial study revealed that after a storage of 12 weeks at 4°C in fluid, no changes of the physico-chemical parameter, like e.g. ζ-potential, volume susceptibility and hydrodynamic size or pH could be found. Likewise, not release of peptide was detected and there was no difference in magnetic removal performance.

Evaluation of changes in cell cycle of different blood cells by SPION-APTES-Pep

Especially, when used in a bypass system to remove pathogens from patient blood for diagnosis of very low microorganism numbers, it is of utter importance that the nanoparticles do not influence the blood cells. Additionally to the earlier performed blood compatibility testing, we now tested the effect of SPION-APTES-Pep on the cell cycle of leucocytes using the cell lines Jurkat, THP-1 and freshly isolated peripheral blood monocytes (PBMCs). The results showed that although we saw interaction and uptake of particles with the PBMCs, they did not induce toxicity or alteration of the cell cycle.

Pathogen Separation and regrowth

For magnetic *C. albicans* separation we tested static and flow conditions (10mL/min). For static conditions, we found an effectivity of up to 82% for aqueous buffer and 55% in citrate stabilized blood. Interestingly, the efficiency was in a similar range under flow conditions with up to 76%.
Regrowth of fungi in culture is particularly difficult from blood, since some blood components reduce it. Interestingly, the regrowth performance of *C. albicans* cells magnetically isolated from blood was strikingly better than the usual procedure. 18h after incubation in fluid culture medium, the samples did show changes in optical density that could be attributed to *C. albicans* growth, while the samples directly taken from blood did not grow during the evaluation period of 24h (Fig 2).

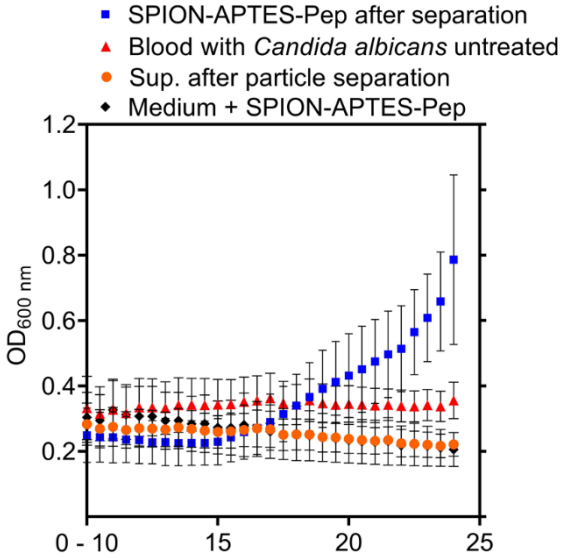

Figure 2. Regrowth of C. albicans in fluid culture with and without magnetic removal from blood.

Conclusion

SPION-APTES-Pep can magnetically remove *Candida albicans* from water-based media and blood after 8 minutes processing highly efficiently under static and flow conditions. Effects on the cell cycle of human blood cells were not found. Moreover, the separated fungal cells could be regrown without any restrictions showing a high potential for an enhanced detection of fungal blood stream infections.

Acknowledgments

The authors thank the DFG SPP1681 and BMBF Diagnoseps for supporting these studies..

References

[1] 1. Delaloye J, Calandra T. Invasive candidiasis as a cause of sepsis in the critically ill patient. Virulence. Jan 1 2014;5(1):161-9.

[2] Herbrecht R, Neuville S, Letscher-Bru V, Natarajan-Amé S, Lortholary O. Fungal infections in patients with neutropenia: challenges in prophylaxis and treatment. Drugs Aging. Nov 2000;17(5):339-51.

[3] Duggan S, Leonhardt I, Hünniger K, Kurzai O. Host response to *Candida albicans* bloodstream infection and sepsis. Virulence. 2015;6(4):316-26.

[4] [5] [6] Friedrich B, Lyer S, Janko C, Unterweger H, Brox R, Cunningham S, Dutz S, Taccardi N, Bikker FJ, Hurle K, Sebald H, Lenz M, Spiecker E, Fester L, Hackstein H, Strauß R, Boccacccini AR, Bogdan C, Alexiou C and Tietze R. Scavenging of bacteria or bacterial products by magnetic particles functionalized with a broadspectrum pathogen recognition receptor-motif offers diagnostic and therapeutic applications. Acta Biomater 2022 Mar; 15;141:418-428. Epub 2022 Jan 7.

Ferroelectrics meet ferromagnets: on the way to liquid multiferroic materials

H. Nádasi[1], M. Küster[2], F. Ludwig[2], A. Eremin[1]

[1] *Institut für Physics, Otto-von-Guericke Universität Magdeburg, 39108 Magdeburg, Germany*
[2] *Institut für Elektrische Messtechnik und Grundlagen der Elektrotechnik und LENA, TU Braunschweig, Braunschweig, Germany*

Liquid suspensions of sphere- and rod-shaped ferromagnetic nanoparticles do not show any ferromagnetic behaviour independently of whether the host is isotropic or anisotropic (liquid crystal). In 2013, it was demonstrated that the suspensions of the scandium-doped barium hexaferrite ScBaHF nanoplatelets in a nematic liquid crystal form a ferromagnetic fluid [1]. The ferromagnetic order of the nanoplatelets is believed to be stabilised by the nematic director coupled to the particles via the director anchoring. Later it was demonstrated that the ferromagnetic order does not require the liquid crystal (LC) host and can be achieved in an isotropic environment [2]. At sufficiently high concentrations, ScBaHF nanoplatelets form colloidal nematics in n-decane and show ferromagnetic properties [2,4,5]. Another important breakthrough in the last few years was the discovery of true 3D ferroelectric liquids. Due to the polar symmetry, those liquids are nematic liquid crystals. Although ferroelectric LCs have been known since the sixties of the twentieth century, most of them were of smectic or columnar type, which could not provide a host for the dispersions of nanoparticles. Ferroelectric nematics are distinguished by a for LCs exceptionally high spontaneous polarisation reaching as high as 6 $\mu C/cm^2$, and a large dielectric response [6-8]. Recently, it has been shown that being ferroelectric, such liquids can guide an electric field along curved microchannels or even stabilise freely suspended filaments.

The discovery of ferroelectric nematics also provides a new framework for developing novel hybrid materials combining the ferroelectric and ferromagnetic properties in one liquid.
In this presentation, we demonstrate the feasibility of liquid multiferroics consisting of a ferroelectric nematic host and dispersed magnetic nanoplatelets. We show that such materials exhibit a magneto-electric effect where the magnetic excitation of such materials results in an electric response. Additionally, we characterise the nonlinear optical response, the optical generation of the second harmonic (SHG) resulting from the polar nanostructure of the material.

Acknowledgments

This research was supported by Deutsche Forschungsgemeinschaft via projects NA1668/1, LU 800/7-1, and ER 467/8-3

References

[1] A. Mertelj, D. Lisjak, M. Drofenik, and M. Čopič , Nature 504, 237 (2013).
[2] M. Shuai et al., Nature Comm. 7, 10394 (2016).
[3] A. Mertelj and D. Lisjak, Liq Cryst Rev 5, 1 (2017).
[4] M. Küster et al., J Mol Liq 360, 119484 (2022).
[5] H. Nádasi et al., J Mol Liq 382, 121900 (2023).
[6] A. Mertelj et al., Splay Nematic Phase, Phys Rev X 8, 041025 (2018).
[7] N. Sebastián et al., Phys Rev E 106, 021001 (2022).
[8] E. Zavvou et al., Soft Matter 18, 8804 (2022).

Electrical properties of magnetorheological fluids

Sushma Raghavendra Rao, Gareth J. Monkman

Mechatronics Research Unit, OTH-Regensburg

Abstract

The phase change form Newtonian fluid to semi-solid in a magnetorheological fluid commences with chain formation of the suspended magnetic particles. The resulting physical effects are not immediate. Response times quoted in the literature vary widely due to the diverse magnetic and dynamic conditions. However, the initial phase change is easily measurable as the onset of chain formation results in abrupt changes in electrical properties. This work concerns the analysis of electrical properties, including capacitance, resistance and the respective time constants for magnetorheological fluids based on carbonyl iron powder suspended in silicone oil under mechanically and magnetically static conditions.

Introduction

The mechanical response times of MRF have been measured by several researchers, for example [1]. Rise and fall times differ considerably within the range 0.25 ms to 1 s. However, in almost all cases, the response time of the complete system including the MRF was determined rather than that of the MRF alone.

The application of a magnetic field results in the physical displacement of magnetic particles suspended in the carrier fluid. This usually occurs in the form of alignment of the particles along the direction of the magnetic flux lines. The magnetic field causes a reduction in inter-particle distance, which results in a measurable increase in electrical capacitance. It is important to note, that only a change in electrical capacitance takes place, not a change in the relative permittivity ε_r of the dielectric material. Consequently, the resulting interfacial magnetocapacitance [2] is not a magnetodielectric effect as the relative permittivity is a function of the molecular structure of the oil or polymer material alone, which remains uninfluenced by the magnetic field [3].

Experimental

Two experimental configurations were employed. The first consisted of two parallel planar electrodes between which the sample fluid was contained. The second comprised a coaxial probe which was immersed in the fluid sample. Measurements of capacitance and resistance for both parallel and series CR circuit characteristics were made using various LCR measurement bridges (Philips PM6303 and Hameg 8118).

Both electromagnet and permanent magnet configurations were used for magnetic field generation with comparable results.

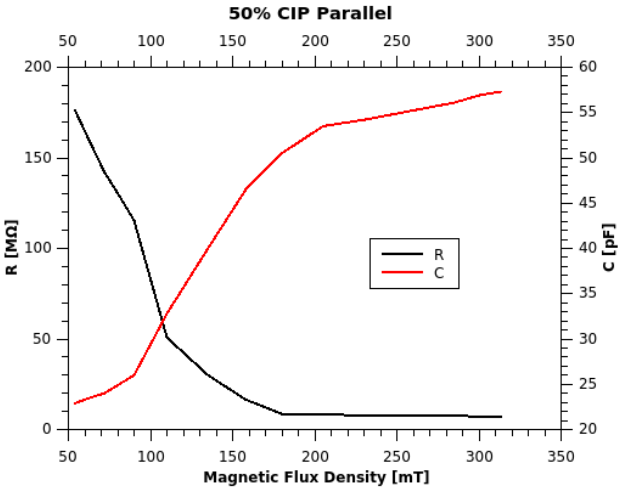

*Figure 1a. Parallel R and C vs. **B** field*

Figure 1a and 1b show the typical characteristics of capacitance and resistance respectively, for the 50% wt. CIP sample MRF. Large amounts of data were gathered using both coaxial probes and planar capacitors. Apart from different offsets, the measurements were effectively identical. For other CIP concentrations the curves are of similar shape but with differing ordinate scales. In order to avoid unnecessary clutter only the 50% wt. CIP curves are shown in figure 1.

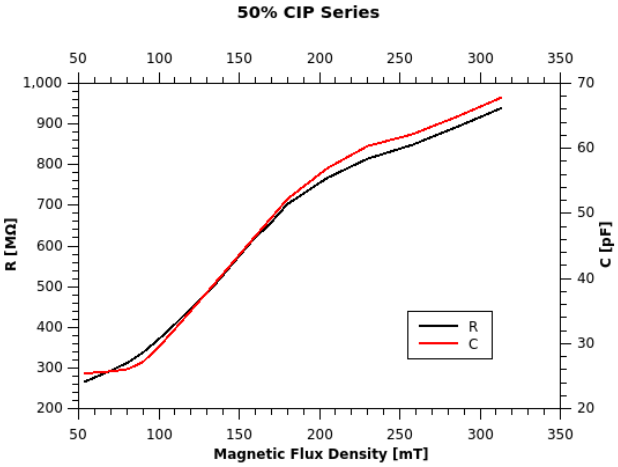

*Figure 1b. Series R and C vs. **B** field*

Observation shows that the parallel CR time constants are very similar regardless of CIP content but reduce significantly with increasing magnetic flux density and tend to a steady-state under 1 ms at flux densities above 200 mT. On the other hand, the series CR time constants are generally longer with similar influence from CIP content but rise almost linearly with increasing magnetic flux density as shown in figure 2 b.

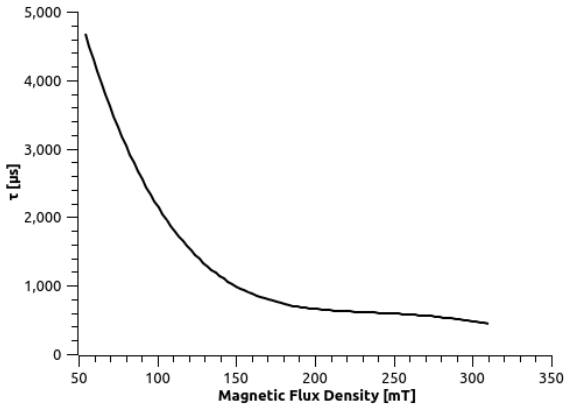

*Figure 2a. Parallel τ vs. **B** field*

Observing the curves of figures 1 and 2, parallel CR time constants commence between about 4 and 6 milliseconds and sink by about an order of magnitude as the magnetic flux density approaches 200 mT. At the same time the series CR time constant undergoes up to a 10-fold increase for the same increase in magnetic flux density.

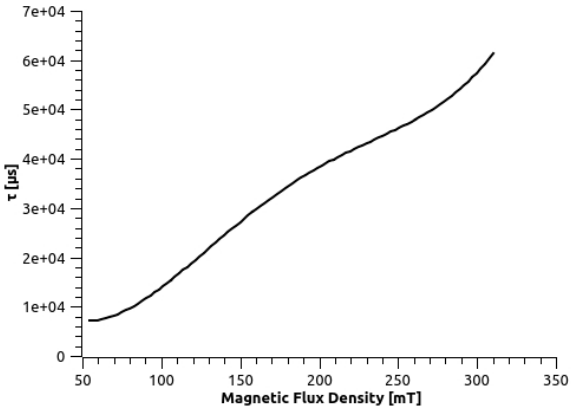

*Figure 2a. Series τ vs. **B** field*

Such measurements can vary considerably depending on the level of CIP suspension in the carrier fluid. The measurements made in this work were conducted immediately following agitation and the data compiled in order to generate figures 1 and 2 are based on numerous measurements and statistical evaluation which accounts for the spread of the curves in figure 2.

Acknowledgements

The authors would like to thank the German Research Federation (DFG) for the grants (MO 2196/2-1) "Investigation of the electrical properties of magneto-active polymers" within SPP1681 and (MO 2196/11-1) "Magneto-rheopectic Boron organo-silicone-oxides (MrBos)" which made this research possible.

References

[1]. Choi. Y-T & N.M. Wereley - Comparative Analysis of the Time Response of Electrorheological and Magnetorheological Dampers Using Nondimensional Parameters - *Journal of Intelligent Material Systems and Structures* Vol. 13—July/August 2002 DOI: 10.1106/104538902028557

[2]. Lawes. G., T. Kimura, C.M. Varma, M.A. Subramanian, N. Rogado, R.J. Cava & A.P. Ramirez - Magnetodielectric effects at magnetic ordering transitions - *Progress in Solid State Chemistry*, *37,* 40-54, 2009.

[3]. Guo. F., C-b. Du, & R-p. Li - Viscoelastic Parameter Model of Magnetorheological Elastomers Based on Abel Dashpot - *Advances in Mechanical Engineering,* 2014.

Magnetic field-driven locomotion systems based on magnetoactive elastomers

M. Reiche[1], L. Zentner[1], D. Borin[2], T.I. Becker[1]

[1] *Mechanics of Compliant Systems Group, Faculty of Mechanical Engineering, Technische Universität Ilmenau, 98684 Ilmenau, Germany*
[2] *Magnetofluiddynamics, Measuring and Automation Technology, Technische Universität Dresden, 01062 Dresden, Germany*

Magnetoactive elastomers (MAEs) have material properties that influence each other in a mutually exclusive manner under magnetic field application. These elastomers consist of a soft elastic matrix filled with hard and/or soft magnetic particles. Micron-sized magnetic particles with a high coercivity, i.e. hard, enable to maintain their magnetization after magnetization in a strong magnetic field. Through this process, an elastic magnet can be created. The use of soft magnetic particles increases the net filling of the MAE, and therefore extends the field-induced variation of its magnetic properties, such as magnetic susceptibility [1,2].

Motion systems based on MAEs show promising potential in the field of soft robotics. Their comparison with robots made of rigid links and joints shows that soft robots based on MAE can be moved with a minimum number of actuators [3]. In this work, we focus on realization of multimodal locomotion systems driven by magnetic fields. Solutions to combine different principles of locomotion in one mobile system are under our consideration.

In particular, we investigate vibration-driven systems based on multipole magnetized MAE for planar locomotion. The MAE in a beam form contains both magnetically hard and soft particles and is magnetized in a way that it has three poles overall with the same poles at the end. An alternating magnetic field of a coil fixed above the MAE beam generates a forced bending vibration of the beam in the vertical plane due to the induced magnetic attractive and repelling forces. The oblique bristles on the underside of the MAE beam are attached to realize asymmetrical friction forces which, in combination with the cyclic inertial forces of bending vibrations, lead to an offset of the support points, and thereby to a system´s propelled movement. The considered system design utilizes simple magnetic actuation that allows to achieve fast motion in a resonant mode. Specific design variations, such as bristle arrangement and application of several MAE beams, enable linear and planar locomotion in different directions with additional features, such as load carrying and obstacle overcoming.

As shown in [4], the locomotion system made of the multipole MAE beam, which has bristles protruding obliquely only in one direction, enables linear movement in the opposite direction. This unidirectional movement depends on the magnetic actuation frequency, whereby the advancing speed reaches a maximum response of 70.4 mm/s at a frequency of 75 Hz.

Adjusting the bristle arrangement in a way that the bristles protrude in different directions at the underside of the MAE beam, allows bi-directional movement of the locomotion system (Fig. 1).

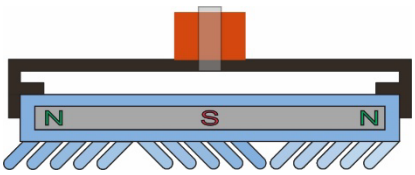

Figure 1. Locomotion system for bi-directional movement.

The system generates linear motion for coil excitation frequencies in the range up to 130 Hz, with the frequency-dependent reverse motion for frequencies between 1-6 Hz, 8-12 Hz, 17-19 Hz, and at 53 Hz. The maximum advancing speed forward is 60.8 mm/s at a frequency of 59 Hz, and the maximum advancing speed reverse is 2.9 mm/s at a frequency of 10 Hz (Fig. 2).

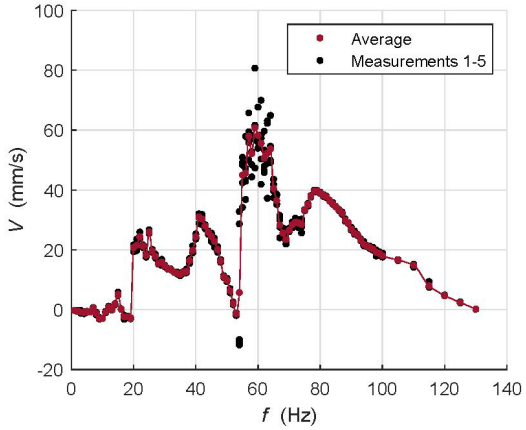

Figure 2. Advancing speed of the locomotion system for horizontal bi-directional movement dependent on the magnetic field excitation frequency.

The vertical motion opposed gravity is achieved by the locomotion system made of two multipole magnetized MAE beams. They are arranged around the actuating coil and have mirror-symmetrical magnetization. Figure 3 shows the system´s upward locomotion between two plexiglass plates. A vertical movement through a tube is also possible.

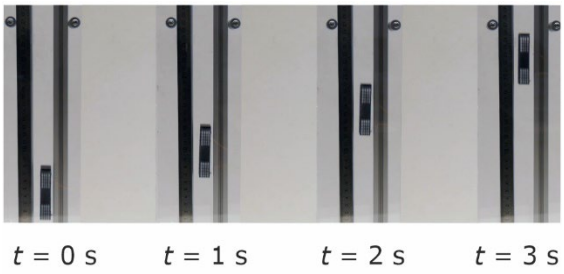

Figure 3. Comparison of distances covered by the locomotion system for vertical movement at an excitation frequency of 75 Hz.

The system moves in the frequency range between 15-170 Hz, whereby a frequency-dependent bi-directional movement is identified. The upward movement against the weight force reaches a maximum speed of 61 mm/s at a frequency of 75 Hz. The downward movement occurs for frequencies between 15-40 Hz and 105-170 Hz with a maximum speed of 1.3 mm/s at an excitation frequency of 105 Hz (Fig. 4).

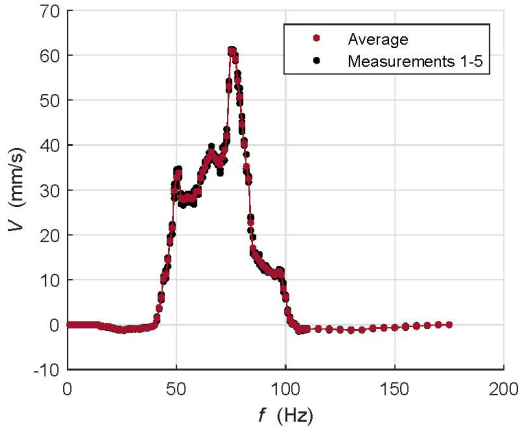

Figure 4. Advancing speed of the locomotion system for vertical bi-directional movement dependent on the magnetic field ex-citation frequency.

Further improvements of the presented systems will be oriented to realize planar locomotion, to make them autonomous concerning energy supply and to improve controlling ability.

Acknowledgments

The work is funded by the Deutsche Forschungsgemeinschaft (DFG), project BE-6553/2-1.

References

[1] T.I. Becker, O.V. Stolbov, A.M. Biller, D.Yu. Borin, O.S. Stolbova, K. Zimmermann, Yu. L. Raikher. Shape-programmable cantilever made of a magnetoactive elastomer of mixed content. Smart Materials and Structures 31 (2022) 105021.

[2] T.I. Becker, O.V. Stolbov, D.Yu. Borin, K. Zimmermann, and Yu.L. Raikher. Basic magnetic properties of magnetoactive elastomers of mixed content. Smart Materials and Structures 29 (2020) 075034.

[3] J. Chavez, V. Böhm, T.I. Becker, S. Gast, I. Zeidis, and K. Zimmermann. Actuators based on a controlled particle-matrix interaction in magnetic hybrid materials for applications in locomotion and manipulation systems. Physical Sciences Reviews 7(11) (2022) pp. 1263-1290.

[4] M. Reiche, T.I. Becker, G.V. Stepanov, K. Zimmermann. A multipole magnetoactive elastomer for vibration-driven locomotion. Soft Robotics 10(4) (2023) pp. 770-784.

Ferronematic phases based on liquid crystalline polymer decorated barium hexaferrite nanoparticles

B. Rhein[1], G. Richwien[1], A. M. Schmidt[1], J. Kopp[2] and J. Landers[2]

[1]Department Chemistry, Institute for Physical Chemistry, University of Cologne, Greinstraße 4-6, 50939 Cologne
[2]Faculty of Physics and Center for Nanointegration Duisburg-Essen (CENIDE), University of Duisburg-Essen

Molecular liquid crystal (LC) materials have gained significant prominence in modern electronics, including displays and sensors, as well as in materials science for applications like soft robotics. In these applications, control occurs primarily by electric fields or temperature changes [1]. Despite the principal potential for a direct manipulation of pure LCs by means of magnetic fields, which would open a large number of novel applications, the required magnetic field strengths are too high to be conveniently accessible [2]. In 1970, Brochard and de Gennes proposed the concept of achieving magnetic control over molecular LC phases by dotation with magnetic nanoparticles. Despite the exact mechanism of the magnetic-nematic interaction still being under debate, since 2013 several systems have been reported to achieve a reduction in the threshold of the magnetic field strength for the Fréedericksz transition by several magnitudes [3]. In these systems, a direct coupling of the nematic and magnetic directors is experimentally confirmed, resulting in the creation of ferromagnetic properties in liquids at room temperature [3]. However, the successful integration of magnetic nanoparticles into LC phases is met with challenges such as nanoparticle agglomeration, or even complete phase separation between the magnetic and nematic components [4]. To overcome those challenges, and to develop a versatile strategy for the enhancement of the compatibility between different, (including magnetic) nanoparticle dopants and the molecular LC phase, the functionalization of the particle surface with help of surfactants or polymers is considered [2],[5]. The present work focuses on the covalent surface functionalization of barium hexaferrite nanoplatelets with mesogen decorated, polymethylsiloxane-based polymer brushes. The covalent attachment of a high number density of nonyloxycyanobiphenyl (9OCB) units via flexible tethering aims to increase the dopants compatibility with the surrounding LC phase composed of 4-cyano-4'-pentylbiphenyl (5CB), and to promote a successful anchoring with the nematic phase.

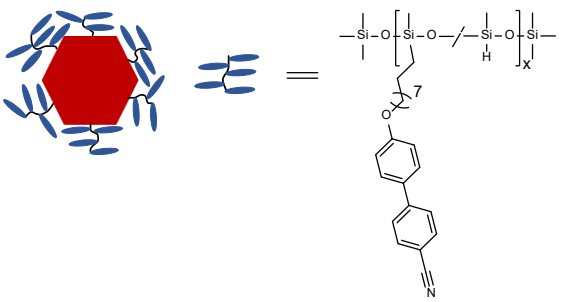

Figure 1. Functionalized Barium hexaferrite nanoplatelets with a polymer brush consisting of 9OCB and PHMS.

To comprehensively characterize these systems, a bouquet of

complementary analytical techniques is employed, including transmission electron microscopy, magnetometry, elemental analysis, and differential scanning calorimetry. Beyond addressing challenges related to nanoparticle dispersion and compatibility, this research also delves into compatibility issues and coupling mechanisms inherent to such systems. In future experiments, we aim to elucidate the potential of further refinement in terms of dopant concentration, nanoplatelet morphology, and polymer brush chemistry.

References

[1] T. Kato, J. Uchida, T. Ichikawa, T. Sakamoto, *Angewandte Chemie - International Edition* 2018, *57*, 4355–4371.

[2] K. Koch, M. Kundt, A. Eremin, H. Nádasi, A. M. Schmidt, *Physical Chemistry Chemical Physics* 2020, *22*, 2087–2097.

[3] F. Brochard, P. G. de Gennes, *Journal de Physique* 1970, *31*, 691–708.

[4] M. Hähsler, I. Appel, S. Behrens, *Physical Sciences Reviews* 2020, DOI 10.1515/psr-2019-0090.

[5] K. Koch, M. Kundt, A. Barkane, H. Nádasi, S. Webers, J. Landers, H. Wende, A. Eremin and A. M. Schmidt, *Physical Chemistry Chemical Phyics*, 2021, 23, 24557–24569.

Progress in modeling magneto active elastomers

D. Romeis[1], M. Roghani[1], M. Saphiannikova[1]

[1] *Leibniz-Institut für Polymerforschung Dresden, Germany*

Magnetic hybrid materials made of magnetizable microparticles embedded in an elastomeric matrix are called Magneto Active Elastomers (MAEs). Due to strong magneto-mechanical coupling on short and long length scales a general characterization of their material behavior is very challenging.

We developed a powerful mean-field dipole approach [1, 2] that captures various aspects of the intrinsic magneto-mechanical interplay. The formulation allows to account simultaneously for the microscopic particle distribution and macroscopic sample form. In this way, an analytic approximation for the effective magnetization behavior in MAEs [3], spanning from linear to saturation regime, for isotropic and anisotropic particle arrangements is derived. The results clearly reveal that anisotropic particle distributions have an equivalent effect as anisometric sample shapes. Furthermore, our approach enables an efficient characterization of magnetization fields in real-sized samples that can be implemented in macro-continuum models.

Evolution of microstructure caused by an applied magnetic field is another fascinating phenomenon with a significant impact on the mechanical behavior of MAEs. We just presented a model that captures the microstructure evolution and its effect on the mechanical properties with a small number of model parameters [4]. A penalty term is introduced to compensate for the micro-mechanical elastic energy required to move the particles inside the cross-linked elastomer. Our results predict a huge increase in the elastic modulus of MAEs made of a very soft elastomeric matrix. The magneto-rheological effect is accompanied by non-monotonic elongation of samples. The model parameters can be modified to adjust the behavior to specific materials and testing procedures used in the experiments. Validation for cylindrical samples is presently in progress.

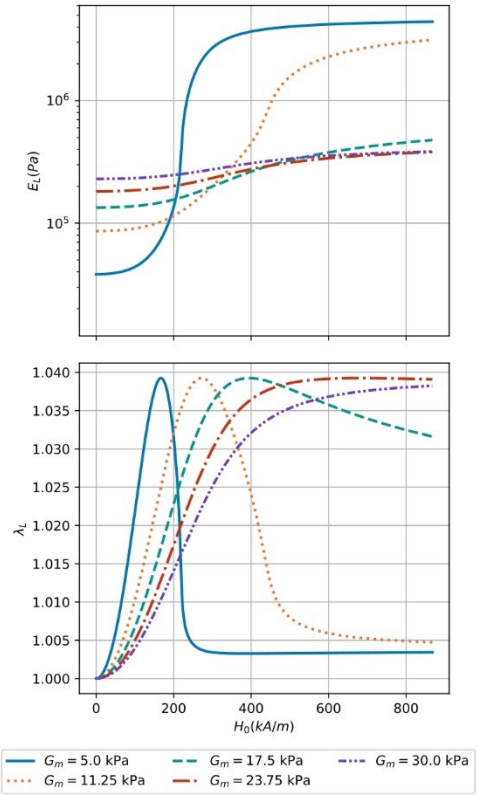

Acknowledgments

Financial support by German Research Foundation research project 380321452/ GRK2430 is gratefully acknowledged.

References

[1] D. Romeis, M. Saphiannikova, A cascading mean-field approach to the calculation of magnetization fields in magnetoactive elastomers, *Polymers*, 13: 1372 (2021).

[2] S. Chougale, D. Romeis, M. Saphiannikova, Magneto-mechanical enhancement of elastic moduli in magnetoactive elastomers with anisotropic microstructures, *Materials*, 15: 645 (2022).

[3] D. Romeis, M. Saphiannikova, Effective magnetic susceptibility in magnetoactive composites, *J. Magn. Magn. Mat.*, 565: 170197 (2023).

[4] M. Roghani, D. Romeis, M. Saphiannikova, Effect of microstructure evolution on the mechanical behavior of magneto-active elastomers with different matrix stiffness, *Soft Matter*, 19: 6387 (2023).

Magnetic nanoparticles pass a differentiating *in vitro* blood-placenta barrier

S. Schapp[1], P. Radon[2], A. Trinks[1], D. Zahn[3], F. Wiekhorst[2], S. Dutz[3,4], A. Hochhaus[1], J.H. Clement[1]

[1] *Klinik für Innere Medizin II, Abt. Hämatologie & Internistische Onkologie, Universitätsklinikum Jena, Am Klinikum 1, D-07747 Jena, Germany; mail: joachim.clement@med.uni-jena.de*
[2] *Physikalisch-Technische Bundesanstalt, Berlin, Germany*
[3] *Institut für Biomedizinische Technik und Informatik (BMTI), Technische Universität Ilmenau, Germany*
[4] *Leupold-Institut für Angewandte Naturwissenschaften (LIAN), Westsächsische Hochschule Zwickau, Germany*

Introduction

The application of nanomaterials in a medical context is rapidly progressing. There is still the necessity to understand the interaction between nanomaterials and the human body in more detail, especially at cellular boarders like the blood-placenta barrier. Since clinical studies in pregnant women are difficult to perform, physiologically appropriate models of the human placenta are needed to study the interactions between nanoparticles and placenta *in vitro*.
The placenta delivers nutrients from the maternal blood to the fetus and eliminates metabolites in reverse direction. This organ is essential to protect the fetus from harmful substances. Various cell types are involved in building up the blood-placenta barrier (BPB), especially trophoblasts and endothelial cells, placental macrophages and pericytes. During pregnancy, the placenta is highly dynamic in its morphology and composition, e.g. the cytotrophoblasts fuse and form the syncytiotrophoblast.
The aim of our investigations is to gain a better understanding of the interactions of magnetic nanoparticles (MNP) with the blood-placenta barrier. We could show previously, that the coating and the surface charge of MNPs affect the passage through an *in vitro* blood–placenta barrier under fluidic conditions in a microfluidic biochip [1,2]. In the present study, we investigated whether the fusion of cytotrophoblasts to syncytiotrophoblasts affects MNP passage through the barrier.

Materials and Methods

The in vitro BPB was established in a microfluidic chip (microfluidic chipshop, Jena) by using the cytotrophoblast cell line BeWo on the apical (maternal) side and human primary placental pericytes on the basolateral (fetal) side (Figure 1) [1]. Differentiation of the BeWo cells was induced by supplementation of the medium with 20 µM forskolin for 24h. This treatment was repeated as indicated.

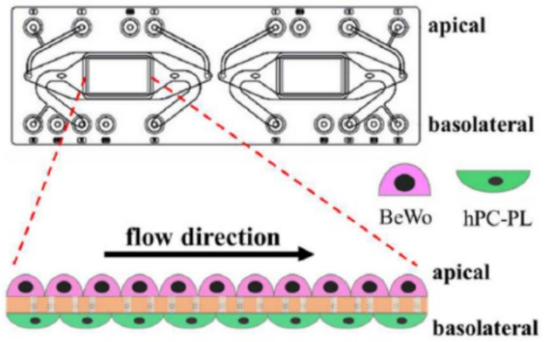

Figure 1. Schematic representation of the BPB in the microfluidic chip and the localization of BeWo cells and pericytes (hPC-PL).

Molecular permeability assays using sodium fluorescein were conducted to prove cell barrier integrity prior to MNP incubation. The differentiating agent forskolin (dissolved in DMSO) was applied up to 3 times in 24h periods with a concentration of 20 µM. Forskolin-induced differentiation of the BeWo cells was evaluated by qPCR (LGALS13, ZO-1, CGB1, SPTAN1). Morphological changes were monitored by immunofluorescence staining of the tight junction-associated protein ZO-1 of BeWo cells. Citrate-coated MNP (hydrodynamic diameter 134 nm, ζ-potential -51 mV) were applied for 24h (final concentration in the apical compartment 100 µg/ml). For quantification of the MNP content in the apical and basolateral compartment as well as in the cell layer magnetic particle spectros-

copy (MPS) was performed. For MPS, the third harmonics of the spectra were normalized to the moment of a MNP reference sample of known iron amount. Cytokine release was measured with the LEGENDplex human inflammation assay (BioLegend™, San Diego, USA) and for selected cytokines with ProQuantum Immuno-Assays (Thermo Fisher Scientific, Osterode).

Results and Discussion

BeWo cells co-cultured with pericytes form a stable barrier inside the microfluidic biochip. In order to simulate the changes of the placenta during pregnancy we used forskolin (F) as a differentiating agent for the BeWo cells (cytotrophoblasts). In consequence, the cells are forced to fuse and form syncytiotrophoblasts, which are dominant in the late stage of pregnancy *in vivo*. This differentiation process is accompanied by altered gene expression and subsequent morphological changes. The expression of the pregnancy hormone Choriogonadotropin beta (CGB) was significantly upregulated (log2 ratio +5.3 ± 0.4 (3xF; $p < 0.001$), +4.2 ± 1.0 (2xF; $p < 0.01$), +3.8 ± 1.1 (1xF; $p < 0.01$)), whereas ZO-1 expression was reduced compared to untreated samples (log2 ratio -0.8 ± 0.4 (3xF; $p < 0.05$), -1.4 ± 0.3 (2xF; $p < 0.01$), -1.1 ± 0.2 (1xF; $p < 0.05$). This was confirmed by immunofluorescence staining. Even after a single forskolin incubation for 24h BeWo cell boarders are largely disrupted (Figure 2).

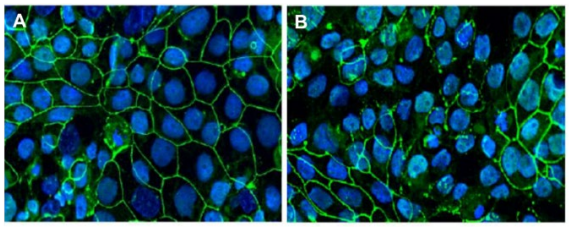

Figure 2. A: Untreated BeWo cells with well-structured and tight cell borders (green). B: BeWo cells after treatment with 20 µM forskolin for 24h to induce cytotrophoblast fusion. Cell membranes are largely degraded (green dots). Cell nuclei are stained with DAPI (blue); Cell membranes are stained with ZO-1 (green). Magnification 20x.

After forskolin (2xF) and MNP incubation the MNP content in the apical and basolateral compartment was determined by MPS. The penetration rate of MNPs was not affected by the formation of syncytiotrophoblasts. In the basolateral compartment, no significant difference in MNP content was measured between DMSO (control) (3.8% ± 4.9%) and 2-times forskolin treated samples (4.2% ± 2.7%) (Figure 3).

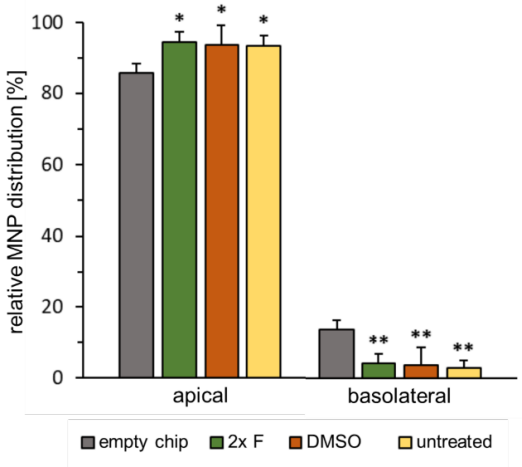

*Figure 3. Relative MNP distribution in the BPB after double forskolin incubation (n=3); * p<0.05;** p<0.01.*

Finally, we studied the secretion of a panel of 13 cytokines after a 2-times forskolin and MNP incubation to monitor putative inflammatory effects. IL-6, IL-8 and MCP-1 were the predominant cytokines. The IL-6 release was enhanced 2-fold after forskolin and MNP treatment.

Conclusion and Outlook

We show that citrate-coated MNPs pass a syncytiotrophoblast to a similar extent as a cytotrophoblastic cell layer. This will allow further studies on the passage of MNPs through a late stage blood-placenta barrier.

Acknowledgement

We thank Cornelia Jörke for expert technical assistance. This work was supported by Deutsche Forschungsgemeinschaft (DFG) in the framework of the priority program 1681 (CL202/3-3, DU1293/7-3, WI4230/1-3).

References

[1] Gresing, L., et al. *J Magn Magn Mater* 2021; 521: 167535
[2] Gräfe, C., et al. *Phys Sci Rev* 2022; 7: 1443-1500

Synthesis and characterization of magnetoplasmonic $CoFe_2O_4$ @Au-NPs in a thermo-responsive polymer matrix

P. Schütz[a], S. Lemich[a] , M. Weißpflog[a] , P. Körner[a], V. Abetz[a,b] and B. Hankiewicz[a]

[a]*Institute of Physical Chemistry, University of Hamburg, Grindelallee 117, 20146 Hamburg, Germany*
[b]*Institute of Membrane Research, Helmholtz-Zentrum Hereon, Max-Planck-Straße 1, 21502 Geesthacht, Germany*

Due to their unique properties, nanomaterials started to gain interest in multiple application fields like sensing, biomedicine, catalysis, or even as a part of composite bulk materials. Nanoparticles (NPs) can be made even more versatile in their properties by combining multiple different materials into one hybrid material. An example of such a hybrid are magnetoplasmonic NPs. These are hybrid NPs made out of a superparamagnetic core such as magnetite or other ferrites that are encapsulated in a gold shell or decorated with gold NPs. The addition of the gold shell adds the plasmonic properties and catalytic activity of the nanostructured gold to the magnetic fluid and additionally increases the stability of MNPs against dissolution and oxidation [1].

These "magnetic gold particles" can be localized in a specific area by magnetic fields and thus improve the application for example in biomedicine compared to ordinary gold NPs, which diffuse in the biological system. The abovementioned properties make the MNP@Au-NPs an interesting alternative to ordinary MNPs or gold NPs and open up different applications utilizing the properties of both components [2]. Additionally, the properties of the hybrid are strongly dependent on the ligands that are used and play an integral part in the possible application of the system. Due to the affinity of thiols to the gold shell, a variety of ligands can be used for these magneto-plasmonic NPs. In this work, polymer ligands are used since they are a versatile ligand class that can add colloidal stability to the system, enable biocompatibility, introduce properties like stimuli-responsiveness, and finally turn colloidal systems into bulk material [3].

To achieve this flexibility and be a reliable ligand for different applications, a highly reproducible and versatile synthesis of the polymer is mandatory. This can be realized using controlled radical polymerization techniques like reversible addition-fragmentation chain-transfer (RAFT) polymerization. Using this approach specific copolymer architectures, chain lengths and degrees of functionalization of the polymers can be tailored to support the particle system for specific applications [4]. In our work, we present a novel synthesis route of multi-responsive hybrid materials based on magnetoplasmonic $CoFe_2O_4$ @Au-NPs inside of a responsive polymer matrix. The synthesis of the hybrid NPs is based on a two-step approach. In the first step, spherical CF-NPs were synthesized via a coprecipitation method and functionalized with different ligands. The ligands on the CF surface were used in situwith the Au(III) precursor to form gold-decorated CF-NPs. Using an additional reducing agent, fully gold-coated CF@Au-NPs were synthesized. Both hybrid nanostructures were then functionalized with a thermo-responsive RAFT polymer without further modification of the polymer using the trithiocarbonate endgroups to achieve the final CF@Au@Polymer hybrid material.

The obtained hybrid material was characterized regarding its magnetic, plasmonic and thermo-responsive properties and compared to these of the components that make up the hybrid material. Investigations showed that the hybrid material exhibits the desired magnetic behavior, plasmonic properties as well as thermo-responsive properties of the polymer matrix. Finally, NIR-irradiation was used to

show that the thermo-responsive phase transitions of the polymer can be triggered using photothermal heating of the particle system. This enables potential applications in drug release and control of the swelling behavior of a hydrogel via NIR-irradiation and the resulting photothermal heating.

Finally, our investigations reveal a synthesis route to create multi-responsive $CoFe_2O_4$@Au@Polymer hybrid materials using tailor-made polymers with thermo-responsive properties, which can be triggered via photothermal or magnetic heating. Using this approach hybrid materials with different polymer compositions, topologies, and responsive properties can be produced to fit the desired application or create responsive bulk material.

Acknowledgments

This work was funded by the Deutsche Forschungsgemeinschaft (DFG) project "GRK 2536".

References

[1] Carlá, F.; Campo, G.; Sangregorio, C.; Caneschi, A.; Julián Fernández, C. de; Cabrera, L. I. Electrochemical characterization of core@shell CoFe2O 4/Au composite. Journal of Nanoparticle Research 2013, 15 (8). DOI: 10.1007/s11051-013-1813-0.

[2] Yoon, G. J.; Lee, S. Y.; Lee, S. B.; Park, G. Y.; Choi, J. H. Synthesis of iron oxide/gold composite nanoparticles using polyethyleneimine as a polymeric active stabilizer for development of a dual imaging probe. Nanomaterials 2018, 8 (5). DOI:10.3390/nano8050300.

[3] Lemich, S. B.; Sobania, N.; Meyer, N.; Schütz, P.; Hankiewicz, B.; Abetz, V. Synthesis of Multiresponsive Gold@Polymer-Nanohybrid Materials Using Polymer Precursors Obtained by Photoiniferter RAFT Polymerization. Macromolecular Chemistry and Physics 2022, 2200355. DOI: 10.1002/macp.202200355.

[4] Xu, J.; Abetz, V. Double thermoresponsive graft copolymers with different chain ends: feasible precursors for covalently crosslinked hydrogels. Soft Matter 2022, 18 (10), 2082–2091. DOI: 10.1039/d1sm01692j.

Active dipolar colloids: interplay of chain formation, phase separation and flocking

Elena Sese-Sansa[1], Demian Levis[2], Ignacio Pagonabarraga[2], Guo-Jun Liao[1], Sabine H.L. Klapp[1]

[1]*Institute of Theoretical Physics, Technical University Berlin, Hardenbergstrasse 36, 10623 Berlin*
[2]*Departament de Fisica de la Matria Condensada, Universitat de Barcelona, Mart i Franqus 1, E08028 Barcelona, Spain*

The dynamical behavior of ”active” (or ”self-propelled”) particles that can convert energy from an internal source or the surroundings into motion, has become a major focus in statistical physics and soft matter sciences. Indeed, it is now well established that active motion, combined with different types of particle-particle interaction, can lead to remarkable collective behavior such as motility-induced phase separation (MIPS), swarming, and vortex formation. Moreover, activity can lead to unusual material properties such as spontaneous flow and odd elastic response. A standard model of active motion is the ”active Brownian particle” (ABP), where each particle moves with a constant propulsion speed along a direction subject to white noise, and the interactions are purely steric and isotropic. Here we consider, as an extension of that model, active particles with dipole-dipole interactions stemming from intrinsic (permanent) dipole moments or dipoles induced by an electric or magnetic field. Realistic examples include ferromagnetic ”rollers” con-fined to a fluctuating surface which may exhibit swarming or vortex patterns when energized by an external (alternating) field [1, 2], magnetotactic bacteria [3], and active metallodielectric Janus particles [4, 5].

We have performed Brownian Dynamics simulations in two dimensions, considering a wide range of motilities and dipolar coupling strengths [7, 8]. At low densities and low motilities, the most important structural phenomenon is the aggregation into chains, very similar to conventional (passive) dipolar particles. Upon increasing the particle mobility, these chain-like structures break, and the system transforms into a weakly correlated isotropic fluid. At intermediate densities and large motility we observe motility-induced phase separation (well established for non-dipolar ABPs) which becomes, however, sup-pressed upon increase of the dipolar coupling. To better understand this phenomenon we have developed a hydrodynamic theory [8] derived by explicitly coarse-graining the microscopic Langevin dynamics, thus allowing for a mapping of the coarse-grained model and particle-resolved simulations. The theoretical approach indeed captures the suppression of MIPS. Moreover, the analysis of the numerically obtained, angle-dependent correlation functions sheds light into the underlying microscopic mechanisms leading to the destabilization of the homogeneous phase. Finally, at high densities, the phase separation disappears, and the system displays a ferromagnetic ”flocking” state, where particles form giant clusters and move collective along one direction. We provide arguments for the emergence of the flocking behavior, which is absent in the passive dipolar system. We close by discussing some open questions.

Acknowledgments

We gratefully acknowledge financial support from the German Research foundation via the Priority Program SPP 1681 during earlier stages of this research.

References

[1] A. Kaiser, A. Snezhko and I. S. Aranson, Sci. Adv., 2017, 3, e1601469.

[2] G. Steinbach, M. Schreiber, D. Nissen, M. Albrecht, E. Novak, P. A. Sanchez, S. S. Kantorovich, S. Gemming and A. Erbe, Phys. Rev. E, 2019, 100 , 012608.

[3] F. Meng, D. Matsunaga and R. Golestanian, Phys. Rev. Lett., 2018, 120, 188101.

[4] S. Gangwal, O. J. Cayre, M. Z. Bazant and O. D. Velev, Phys. Rev. Lett., 2008, 100, 058302.

[5] F. Kogler and S. H. L. Klapp, EPL, 2015, 110, 10004.
H. F. Guzman-Lastra, A. Kaiser and Löwen, Nat. Commun., 2016, 7, 13519.

[6] G.-J. Liao, C. K. Hall, and S. H. L. Klapp, Soft Matter, 2020, 16, 2208.

[7] E. Sese-Sansa, G.-J. Liao, D. Levis, I. Pagonabarraga, and S. H. L. Klapp, Soft Matter, 2022, 18, 5388.

[9] G.-J. Liao, S. H. L. Klapp, Soft Matter, 2021, 17, 6833.

[10] H. Reinken, S. H. L. Klapp, M. Bär and S. Heidenreich, 2018, Phys. Rev. E 97, 022613.

Integrated hyperthermia application and monitoring for localized drug-release in magnetic particle imaging

Thilo Viereck, Klaas-Julian Janssen, Kai Luenne, Meinhard Schilling, and Frank Ludwig

Institute for Electrical Measurement Science and Fundamental Electrical Engineering (EMG), TU Braunschweig, Braunschweig, Germany

Magnetic Particle Imaging (MPI) is a fast and sensitive imaging modality with high contrast, which is well suited as a potential theranostic platform. Especially a combination of MPI with magnetic hyperthermia heating via ac hysteresis losses in magnetic nanoparticles (MNPs) is an appealing strategy. Here, we aim for a spatially focused (localized) and controlled drug release (of drugs with low molecular weight) via a temperature-induced (burst) release mechanism.

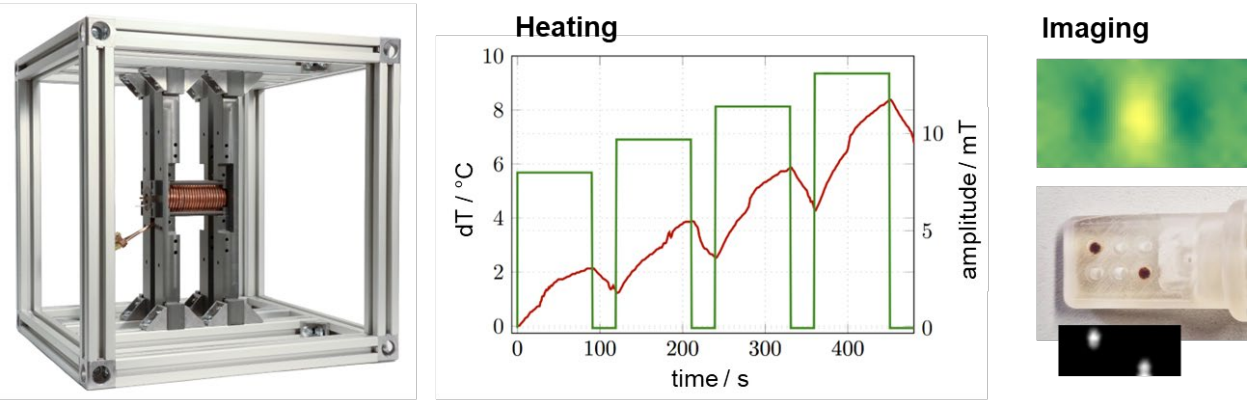

Figure 1. Integrated MPI and magnetic hyperthermia setup (left) enables controlled ac heating (middle) and high-resolution imaging (right).

Compared to hyperthermia for cancer treatment, which typically heats the malicious tissue directly, triggering drug release requires equally high heating power but with minimal duty cycle, i.e. pulsed heating. We are generating sufficient heat around the magnetic nanoparticles to trigger release but without excess heating of the surrounding medium or tissue.

MNP-local heating requires fast and precise temperature monitoring and feedback to meet the designated release temperature. Integrated MPI and magnetic hyperthermia reuses the drive field for both magnetic heating and spatial imaging for monitoring and treatment controlBuilding on previous work, which focused on "functional MPI", including temperature measurements [1] and dual-frequency MPI for spatially resolved particle mobility tracking [2-3], we first designed a magnetic particle spectroscopy (MPS) device for initial heating experiments. It operates with a) a classical fiberoptic temperature probe to obtain SAR/SLP values from calorimetric measurements and b) temperature measurements directly from the MNP

magnetization signal, allowing cross-validation of both temperature measurement techniques. It also enables fast direct feedback from the magnetically obtained temperature signal to achieve feedback control in MPS and to target the release temperature of modified MNPs.
We also successfully implemented ac heating and imaging into a fully integrated prototype MPI system, which will allow temperature monitoring and control for drug release studies on mice shortly.

References

[1] K. J. Janssen, J. Zhong, T. Viereck, M. Schilling, and F. Ludwig, "Quantitative temperature visualization with single harmonic-based magnetic particle imaging", J. Magn. Magn. Mater. 563, pp. 169915, 2022. DOI: 10.1016/j.jmmm.2022.169915

[2] S. Draack, M. Schilling, and T. Viereck, "Magnetic particle imaging of particle dynamics in complex matrix systems", Phys. Sci. Rev. 8(2), 123, 2021. DOI: 10.1515/psr-2019-0123

[3] S. Draack, F. Ludwig, M. Schilling, and T. Viereck, "Dynamic gelation process observed in Cartesian magnetic particle imaging", J. Magn. Magn. Mater. 522, pp. 167478, 2021. DOI: 10.1016/j.jmmm.2020.167478

Hyperthermia behavior of ferrite-based magnetic nanoparticles in a thermo-responsive polymer matrix

M. Weißpflog[a], N. Nguyen[a], N. Sobania[a], V. Abetz[a,b], B. Hankiewicz[a]

[a] *Institute of Physical Chemistry, University of Hamburg, Grindelallee 117, 20146 Hamburg, Germany*
[b] *Helmholtz-Zentrum Hereon, Institute of Membrane Research, Max-Planck-Str. 1, 21502 Geesthacht, Germany*

An extensive field in material science is developed by embedding "hard" magnetic nanostructures within an organic "soft" matter [1]. This also involves the comprehensive characterisation of the individual components and the combined materials, especially with regard to their magnetically induced hyperthermia properties. This describes a predominantly Brownian relaxation mechanism by the application of an alternating magnetic field and generation of a temperature increase that depends i.a. on the ambient medium and its viscosity. A possible field of application is the thermotherapy for tumour treatment [2,3]. Furthermore, in combination with responsive matrices, the biocompatibility of the particles can be increased, drug delivery systems can be produced and magnetic nanoparticles (MNPs) can be localized in concentrated form.

For hyperthermia applications, reproducible synthesis routes of MNP with control and adjustment of the structure, size, shape and magnetic properties are key aspects [4–6]. To minimize the adverse side effects on healthy cells, a large amount of heat generated by a small quantity of nanoparticles must be delivered to the tumor cells only. Therefore, particles with large values of saturation magnetization and a high resolution for magnetic imaging are required leading to a strong and efficient response to the external magnetic field. Moreover, by increasing the saturation magnetization values, the control over the movements of the MNP can be optimized by the external magnetic field after injection into the bloodstream so the required therapeutic concentration of MNP can be reduced accordingly. Among the ferrites, cobalt ferrite ($CoFe_2O_4$) has turned out to be an interesting material as spherical cobalt ferrite shows a higher magnetocrystalline anisotropy than iron oxide [7,8]. As the reduction of the Co 2+ ion concentration in cobalt ferrite particles leads to an increase in average crystallite size, coercivity, and saturation magnetization [7,9,10], our work is focused on the synthesis of nonstoichiometric cobalt ferrite nanoparticles. In a twostep reaction, akageneite nanorods (an antiferromagnetic iron oxide hydroxide) were prepared first followed by an aqueous hydrothermal reaction without toxic surfactants or solvents and variation of the metal salt concentration and composition of $Co^{2+}/Fe^{3+}/Fe^{2+}$. Afterwards, the MNPs were stabilised with citrate ligands to achieve more safety for biological applications.

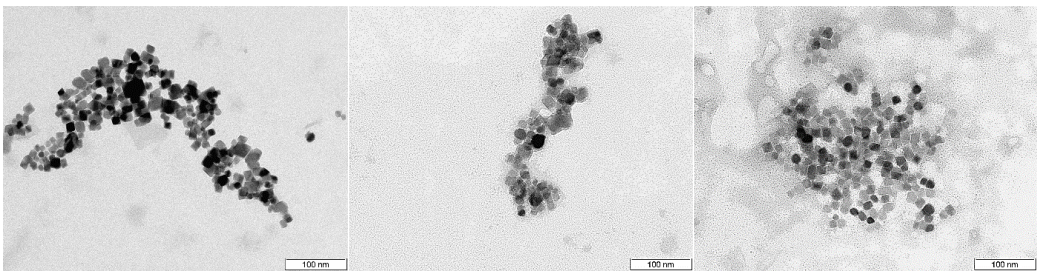

Figure 1. TEM images of selected ferrite-based particles by using different molar ratios of akaganeite to metal salts. The scale bar shows 100 nm for the TE micrographs. The hydrothermal step was carried out with a molar ratio of akaganeite to metal salts ($Co^{2+}/Fe^{3+}/Fe^{2+}$) of (A) 2, (B) 1 and (C) 0.5.

To explore the effect of the cobalt ion concentration and the pressure within the hydrothermal step, magnetic measurements were validated in dependency to size, shape, composition, and structure of the samples. The crystallographic composition of the particles was confirmed by X-ray diffraction and inductively coupled plasma atomic emission spectroscopy.
Cubic and spherical $Co_xFe_{3-x}O_4$ nanoparticles ($0.2 < x < 0.4$) synthesized by molar ratios of akaganeite to metal salts of 0.2 to 2 showed a saturation magnetization of around 15 Am^2/kg to 75 Am^2/kg. It can be observed that an increased Co^{2+} content in the crystals leads to higher crystalline anisotropy, respectively saturation magnetization. Although, the lowest coercivity value could be indicated with highest cobalt ion amount. It was found that the internal lattice strain obtained from the Williamson-Hall plot increases with the pressure within the hydrothermal step due to the successful doping of the crystals with Co^{2+}. This effect can be referred to the smaller atomic radii of Co^{2+} compared to Fe^{2+}. Furthermore, the hyperthermia behavior of the nanoparticle suspensions was carried out at frequencies and magnetic field strengths which results in $H_0 \cdot f < 5 \cdot 10^9$ $A \cdot m^{-1} \cdot s^{-1}$. The highest temperature change at a frequency of 10 kHz and a magnetic field strength of 24.4 mT was determined by the sample synthesized with a molar ratio of 2 and a pressure of 1 bar. $Co_{0.34}Fe_{2.66}O_4$ with an average particle diameter of 18.9 nm leads to a raise up to 9.9 K which means an increase of 80% compared to the 10 mg/mL $Co_{0.80}Fe_{2.20}O_4$ suspensions with an average diameter of 17.6 nm. The SAR value of 45 W/g at given frequency and field strength is up to ten times higher than of stochiometric cobalt ferrite nanoparticles synthesized by precipitation [11]. By increasing the frequency to the value of 150 kHz, the temperature change could be increased to 43 K within 10 minutes while the field strength remained constant ensuring medical applications such as medical imaging and cancer treatment. Finally, we focus on the combination of MNPs with a crosslinkable gel matrix to generate a thermo-responsive ferrogel which may become useful for applications in the field of polymer therapeutics or microactuators. The polymer matrix consists of a double thermoresponsive graft-copolymer which is composed by a poly[oligo(ethylene glycol) methacrylate] backbone and poly(N-isopropylacrylamide) side chains resulting in two segregation temperatures when heated in aqueous solution (lower crictical solution temperature, LCST) [12]. For the synthesis of the polymers, initiator-free photoiniferter reversible addition-fragmentation chain transfer (RAFT) polymerization will be used due to selective initiation of the backbones and side chains from acrylic and methacrylic monomers [13–15]. The number and length of the side chains will significantly influence the mesh size of the gel and, thus, the incorporation of the nanoparticles. In addition, subsequent conversion of the trithiocarbonate pendant groups to thiolreactive functionalities enables further modification and covalently crosslinking with different length of dithiols to afford a thermoresponsive hydrogel or nanostructures embedded hybrid gel. First experiments show the successful embedding of 1.0 to 4.0 % (w/w) of $Co_{0.80}Fe_{2.20}O_4$ in thermo-responsive hydro-gels during the gelation process. These ferrogels have an increased swelling behavior in water compared to the hydrogels. Furthermore, there is a more intense deswelling with temperature during the LCST transition of the polyNIPAM side chains. Hyperthermia measurements of the ferrogels in water show a temperature increase of up to 1.5°C/10 min. Since less than 1/10 of the particle mass was used compared to the ferrofluids, larger amounts of ferrogel as well as a higher particle concentration should increase the temperature effect. This should enable magnetically induced deswelling of the ferrogel promising a potential application in the field of actuator technology and hyperthermia.

Acknowledgments

This work was funded by the Deutsche Forschungsgemeinschaft (DFG) project "GRK 2536". The authors gratefully acknowledge C. Schlundt and N. Schober for measuring XRD as well as S. Werner for measuring TEM. The authors thank the team of the element analysis centre for measuring inductively coupled plasma atomic emission spectroscopy.

References

[1] Tokarev, A.; Yatvin, J.; Trotsenko, O.; Locklin, J.; Minko, S. Adv. Funct. Mater. 2016, 26 (22), 3761–3782.

[2] Hergt, R.; Dutz, S. Journal of Magnetism and Magnetic Materials 2007, 311 (1), 187–192.

[3] Dutz, S.; Hergt, R. Nanotechnology 2014, 25 (45), 452001.

[4] Lemine, O. M. Hybrid Nanostructures for Cancer Theranostics; Elsevier, 2019; pp 125–138.

[5] Leslie-Pelecky, D. L.; Rieke, R. D. Chem. Mater. 1996, 8 (8), 1770–1783.

[6] Lu, A.-H.; Salabas, E. L.; Schüth, F. Angewandte Chemie (International ed. in English) 2007, 46 (8), 1222–1244.

[7] Yasemian, A. R.; Almasi Kashi, M.; Ramazani, A. Mater. Res. Express 2020, 7 (1), 16113.

[8] Fayazzadeh, S.; Khodaei, M.; Arani, M.; Mahdavi, S. R.; Nizamov, T.; Majouga, A. J Supercond Nov Magn 2020, 33 (7), 2227–2233.

[9] Mitra, A.; Mohapatra, J.; Sharma, H.; Aslam, M. Phys. Status Solidi A 2017, 214 (12), 1700505.

[10] Ayyappan, S.; Philip, J.; Raj, B. J. Phys. Chem. C 2009, 113 (2), 590–596.

[11] Lucht, N.; Friedrich, R. P.; Draack, S.; Alexiou, C.; Viereck, T.; Ludwig, F.; Hankiewicz, B. Nanomaterials (Basel, Switzerland) 2019, 9 (12).

[12] Xu, J.; Abetz, V. Soft matter 2022, 18 (10), 2082–2091.

[13] Arrington, K. J.; Matson, J. B. Polym. Chem. 2017, 8 (48), 7452–7456.

[14] Corrigan, N.; Trujillo, F. J.; Xu, J.; Moad, G.; Hawker, C. J.; Boyer, C. Macromolecules 2021, 54 (7), 3430–3446.

[15] Shanmugam, S.; Cuthbert, J.; Kowalewski, T.; Boyer, C.; Matyjaszewski, K. Macromolecules 2018, 51 (19), 7776–7784.

Molecular Dynamics Modeling of Interacting Magnetic Nanoparticles for investigating equilibrium and dynamic assembly properties

M. Wolfschwenger[1*], A. Jaufenthaler[1], F. Hanser[1], D. Baumgarten[1]

[1] *UMIT-Tirol Institute of Electrical and Biomedical Engineering, Hall in Tirol, Austria*
** manuel.wolfschwenger@umit-tirol.at*

Magnetic nanoparticles (MNPs) are of interest for a variety of biomedical applications, e.g. for cancer treatment. A very promising therapy is magnetic drug targeting where magnetic field gradients guide particles to specific sites in the body. There, they can release therapeutic agents, leading to increased drug concentration at the target and reduced systemic toxicity. A precise prediction of the local particle accumulation is required to plan a successful therapy [1]. This is a very challenging task due to several complex flow phenomena. Computational models can provide support to improve the scientific knowledge of those phenomena and act as planning tools.

For this purpose, a variety of macroscopic fluid-flow models describing the particle transport have been developed (e.g. [1]). They can be applied to macroscopic systems but are limited in simulating realistic particle assemblies with all interactions due to the vast number of particles involved. Therefore, microscopic models have been proposed to study the properties of ferrofluids, (e.g. [2]). However, these models do either not consider the micromagnetic behaviour which is responsible for magnetization dynamics as described in [3] or are limited in the variety of interaction potentials.

We aim at developing and validating a model, based on molecular dynamic approaches, that is capable of representing micromagnetic dynamics as well as being used to study equilibrium properties of particle assemblies in viscous media including various interaction potentials.

For our model, we assume all MNPs to be spherical, uniformly magnetized and have uniaxial anisotropy. Each particle has a magnetic core surrounded by a stabilizing surfactant layer. They consist of only one Weiss domain and can therefore be considered as single domain particles with a total magnetic moment. Thus, they can be treated as small magnetic dipoles in a carrier liquid. The solvent is considered as thermally equilibrated at the timescale of the MNP's motion. Thus, the random collisions of the solvent molecules with the MNPs can be modelled as fast fluctuating terms.

The rotational dynamics of the magnetization vectors are described by the stochastic differential Landau-Lifshitz-Gilbert (LLG) equation that is coupled to the differential equation for the physical rotation [3]. The translational motion of the particles is described by Newtons second law.

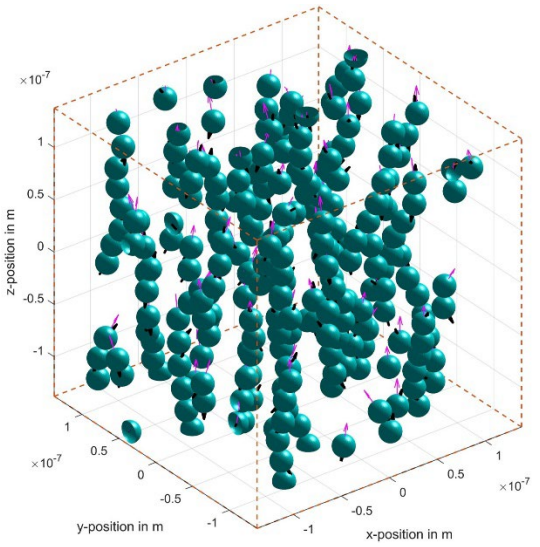

Figure 1. Simulated particle ensemble yielding chain structures

The particles in colloidal systems interact with each other through a number of repulsive and attractive forces. We implemented the attractive van der Waals forces, the magnetic dipole-dipole interactions and the repulsions from the electrostatic double layer and steric interactions.

To compute the interactions between the particles, we use the Ewald summation method, with an error control algorithm. Periodic boundary conditions are employed to study the properties of bulk material. Adaptive timestep solvers with an embedded solution are used to perform the numerical integration of the differential equations. This is important because the dynamics depend on many parameters, making it hard for the user to manually select a proper timestep.

To validate our model we studied the equilibrium and time-dependent properties of a non-interacting particle ensemble and found very good agreement with the theoretical predictions. We observed the expected chain like structures in an interacting system (cf. Fig. 1) too. Also, the error of the dipolar interaction calculation for various Ewald parameters was checked.

The model is currently used to study: the influence of the anisotropy energy constant on the equilibrium magnetization of immobilized particles, the chain size distribution in particle assemblies, temporal properties of interacting particle assemblies and the influence of surface coatings on ferrofluid stability.

References

[1] M. C. Lindemann, et al., *Comput. Methods Programs Biomed.,* vol. 210, 2021.

[2] F. Durhuus, *Nanoscale,* pp. 1970-1981, 2021.

[3] N. Usov and B. Liubimov, *J. Appl. Phys. ,* vol. 112, p. 023901, 2012.

Cobalt ferrite nanoparticles for extracorporeal heating applications

Diana Zahn[1,†], Joachim Landers [2,†], Marco Diegel[3], Soma Salamon[2], Andreas Stihl[4,5], Felix H. Schacher[4,5], Heiko Wende[2], Jan Dellith[3] and Silvio Dutz[1,3,6]

[1] *Institute of Biomedical Engineering and Informatics (BMTI), Technische Universität Ilmenau, Ilmenau, Germany*
[2] *Faculty of Physics and Center for Nanointegration Duisburg-Essen (CENIDE), University of Duisburg-Essen, Duisburg, Germany*
[3] *Leibniz Institute of Photonic Technology (IPHT), Jena, Germany*
[4] *Institute for Organic Chemistry and Macromolecular Chemistry, Friedrich-Schiller-University Jena, Jena, Germany* [5] *Jena Center for Soft Matter (JSCM), Friedrich-Schiller-University Jena, Jena, Germany*
[6] *Leupold Institute for Applied Natural Sciences (LIAN), Westsächsische Hochschule Zwickau, Zwickau, Germany*
[†] *These authors contributed equally to this work*

Introduction

For hyperthermia applications, iron oxide is one of the most common materials for magnetic nanoparticles. Considering technical or biotechnological heating applications in-stead of intracorporeal ones, higher field amplitudes and frequencies can be used, enabling the utilization of particles with larger coercivities (HC). We synthesized high coercivity cobalt ferrite nanoparticles (CoFe-NP) using a wet co-precipitation method and evaluated the correlation of synthesis parameters and resulting particle characteristics in detail. Secondly, we evaluated the effects of different cobalt-to-iron ratios. Particles were characterized using magnetometry, XRD, Mössbauer spectroscopy, TEM and calorimetry. [1]

Methods

CoFe-NP were synthesized by precipitating a solution of $FeCl_2$, $FeCl_3$ and CoCl2 salts with 3M NaOH under constant stirring and defined heating. In a first series of experiments, variations of the following synthesis parameters were evaluated: temperature of the salt solution when adding NaOH (T_{add}), the end temperature the precipitate suspension is heated to (T_{end}), duration of the NaOH addition (dadd) and duration of the overall reaction (d_{react}). Every synthesis was done under air and nitrogen atmosphere. In a second series, synthesis parameters were fixed and the cobalt content x in $CoxFe_3$-xO_4 was varied by changing the ratio of $FeCl_2$ to $CoCl_2$. Every synthesis was done in triplicate. To evaluate the particles' morphology and size, transmission electron microscopy (TEM) images were taken. X-ray diffraction (XRD) measurements were used to evaluate crystal size, lattice parameter a, crystallinity and phase composition. Magnetometry at room temperature (RT) and 5 K up to fields of 9 T was used to determine coercivity HC and magnetization M. Mössbauer spectroscopy was conducted to study the particles' magnetic phase transitions and magnetic alignment behavior. Lastly, calorimetric measurements of 1 wt% particles in fluid or agar at varying field amplitudes and 290 kHz were made.

Results and discussion

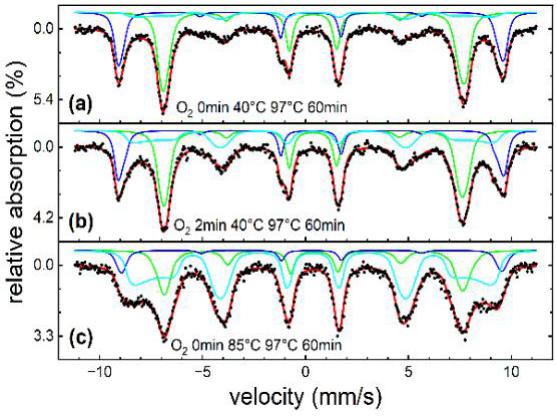

Figure 1. Mössbauer spectroscopy for a sample with low (a) medium (b) and high (c) hydroxide content. The cyan sub-spectrum increases for higher hydroxide content.

Series 1: Correlations between synthesis parameters and particle properties were found as well as thresholds that need to be met to prevent the formation of

crystalline by-phases. For high T_{add} and low T_{end} as well as a d_{add} of 2 and 4 min, crystalline phases other than cobalt ferrite were found by XRD. The formation of a hydroxide, most likely akageneite, was also indicated for some of those multi-phase samples by Mössbauer spectroscopy, leading to an additional subspectrum (fig. 1). Magnetization was found to decrease with increasing hydroxide content (fig. 2 b) and synthesis under nitrogen atmosphere led to higher MRT,2T and lower HC (fig. 2 a).

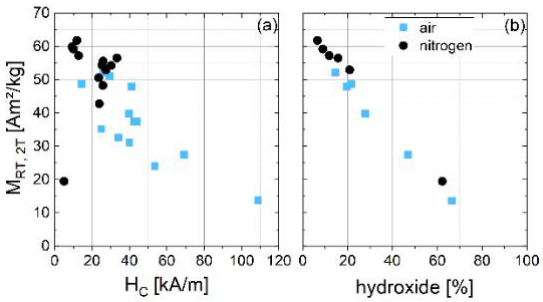

Figure 2. Magnetization at RT and 2 T correlating with HC (a) and hydroxide content (b).

For varying the cobalt fraction x in series 2, the optimized synthesis parameters T_{add} = 40 °C, d_{add} = 2 min, T_{end} = 97 °C and d_{react} = 90 min and nitrogen atmosphere were used.

Series 2: By varying the cobalt fraction, the coercivity of the particles can be tuned (fig. 3 b). The maximum coercivity of 37 kA/m at RT is reached for x = 0.8 – 0.9. Magnetization at 9 T and RT is above 70 Am²/kg with a slight drop for x > 0.9. No crystalline byphases were found in the samples of series 2 due to the optimized synthesis. Particle sizes ranged between 12 and 16 nm with no significant correlation between x and size. Lattice parameter a increased from 8.38 to 8.41 Angström with increasing x.

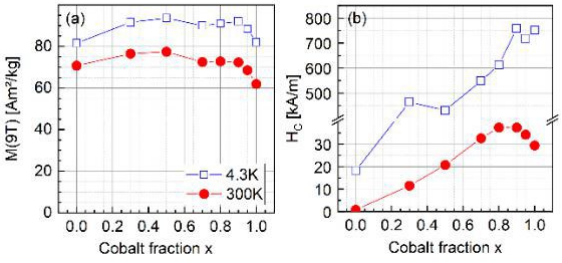

Figure 3. Magnetization at 9 T (a) and HC (b) depending on cobalt fraction x.

Measured SAR of the particles showed a maximum of 480 W/g in fluid and 440 W/g in agar for a cobalt fraction of x = 0.3. For higher x, coercivity was too high to enable an efficient switching of the magnetization with the applied external field amplitudes.

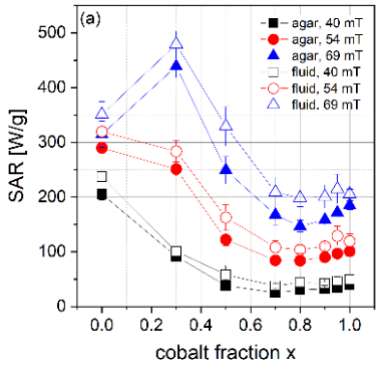

Figure 4. SAR of particles with different cobalt fraction x in fluid and agar.

Conclusion and outlook

We optimized the synthesis of cobalt ferrite nanoparticles with high magnetizations and tunable coercivities that can be used for efficient heating in extracorporeal applications, where high field amplitudes can be used. In ongoing studies, the heating behavior of the particles in a generator with higher field amplitudes is investigated.

Acknowledgements

This work was funded within the "Central Innovation Program for small and mediumsized enterprises" by the Federal Ministry for Economic Affairs and Climate Action of Germany in the project "NanoTherMagS (16KN081337)" and was supported by the "Thüringer Innovationszentrum für Medizintechnik-Lösungen (ThIMEDOP; FKZ 2018 IZN 004). DFG provided funding within the SFB 1278 "Poly-Target" (project number 316213987, project B04), via the CRC/TRR 247 (Project-ID 388390466, sub-project B02) and for the TEM facilities together with the European Fonds for Regional Development (EFRE).

References

[1] Zahn, D.; Landers, J.; Diegel, M.; Salamon, S.; Stihl, A.; Schacher, F.H.; Wende, H.; Dellith, J.; Dutz, S. Optimization of Magnetic Cobalt Ferrite Nanoparticles for Magnetic Heating Applications in Biomedical Technology. Nanomaterials 2023, 13, 1673. https://doi.org/10.3390/nano13101673

List of Participants

Christoph Alexiou
ENT-Clinic/SEON
Universityhospital Erlangen
Waldstrasse 1
91054 Erlangen
Germany
E-mail: christoph.alexiou@uk-erlangen.de

Günter K. Auernhammer
Polymergrenzflächen
Leibniz-Institut für Polymerforschung Dresden e.V.
Hohe Strße 6
1069 Dresden
Germany
E-mail: auernhammer@ipfdd.de

Silke Behrens
Institut für Katalyseforschung und -technologie
Karlsruher Institut für Technologie
Hermann-von-Helmholtz-Platz 1
76344 Eggenstein-Leopoldshafen
Deutschland
E-mail: silke.behrens@kit.edu

Dmitry Borin
Chair of Magnetofluiddynamics, Measuring and Automation Technology
TU Dresden
George-Baehr-Str. 3
1062 Dresden
Germany
E-mail: dmitry.borin@tu-dresden.de

Nils Boussard
E2.6
Universität des Saarlandes
Campus E2.6
66123 Saarbrücken
Deutschland
E-mail: s9nibous@stud.uni-saarland.de

Joachim Clement
Hematology and Internal Oncology
Jena University Hospital
Am Klinikum 1
7747 Jena
Germany
E-mail: joachim.clement@med.uni-jena.de

Charis Czichy
Lehrstuhl für Magnetofluiddynamik, Mess- und Automatisierungstechnik
Technische Universität Dresden
George-Bähr-Straße 3
1069 Dresden
Germany
E-mail: charis.czichy@tu-dresden.de

Sabrina Disch
Fakultät für Chemie
Universität Duisburg-Essen
Universitätsstr. 7
45141 Essen
Deutschland
E-mail: sabrina.disch@uni-due.de

Silvio Dutz
BMTI
TU Ilmenau
G.-Kirchhoff-Str. 2
98693 Ilmenau
Germany
E-mail: silvio.dutz@tu-ilmenau.de

Dietmar Eberbeck
Metrologie magnetischer Nanopartikel
PTB
Abbestrasse 02.Dez
10435 Berlin
Deutschland
E-mail: dietmar.eberbeck@ptb.de

Alexey Eremin
ANP
Otto-von-Guericke-Universität
Universitaetsplatz 2
39106 Magdeburg
Deutschland
E-mail: alexey.eremin@ovgu.de

Arte Feoktystov
Jülich Centre for Neutron Science JCNS at Heinz Maier-Leibnitz Zentrum MLZ
Forschungszentrum Jülich GmbH
Lichtenbergstr. 1
85748 Garching
Germany
E-mail: a.feoktystov@fz-juelich.de

Lukas Fischer
Institut für Physik, Theorie der Weichen Materie / Biophysik
Otto-von-Guericke-Universität Magdeburg
Universitätsplatz 2
39106 Magdeburg
Germany
E-mail: lukas.fischer@ovgu.de

Philipp Gebhart
Institute of Solid Mechanics
TU Dresden
George-Bähr-Straße 3c
1069 Dresden
Germany
E-mail: philipp.gebhart@tu-dresden.de

Marina Grenzer
Institute Theory of Polymers
Leibniz Institute of Polymer Research Dresden
Hohe Strasse 6
1069 Dresden
Germany
E-mail: grenzer@ipfdd.de

Birgit Hankiewicz
Physikalische Chemie
Universität Hamburg
Grindelallee 117
20146 Hamburg
Deutschland
E-mail: Birgit.hankiewicz@uni-hamburg.de

Sofia Kantorovich
Computational and Soft Matter Physics
University of Vienna
Kolingasse 14-16
1090 Vienna
Austria
E-mail: sofia.kantorovich@univie.ac.at

Darshan Kare Gowda
Faculty of Mechanical Science and Engineering Institute of Mechatronic Engineering Chair of Magnetofluiddynamics, Measuring and Automation Technology
Technische Universität Dresden
George-Bähr-Straße 3
1062 Dresden
Germany
E-mail: darshan.kare_gowda@tu-dresden.de

Markus Kästner
Institute of Solid Mechanics
TU Dresden
George-Bähr-Str. 3c
1069 Dresden
Deutschland
E-mail: markus.kaestner@tu-dresden.de

Jens Kirchner
Lehrstuhl für Technische Elektronik
Friedrich-Alexander-Universität Erlangen-Nürnberg (FAU)
Cauerstr. 9
91058 Erlangen
Germany
E-mail: jens.kirchner@fau.de

Sabine Klapp
Institute of Theoretical Physics
Technical University Berlin
Hardenbergstrasse 36
10623 Berlin
Germany
E-mail: sabine.klapp@tu-berlin.de

Juri Kopp
Physics
University Duisburg-Essen
Lotharstraße 1
47048 Duisburg
Germany
E-mail: juri.kopp@uni-due.de

Margarita Kruteva
Jülich Centre for Neutron Science
Forschungszentrum Jülich GmbH
Wilchelm-Johnen Straße -
52425 Jülich
Germany
E-mail: m.kruteva@fz-juelich.de

Joachim Landers
Faculty of Physics
University of Duisburg-Essen
Lotharstr. 1
47057 Duisburg
Germany
E-mail: joachim.landers@uni-due.de

Adrian Lange
Institut für Mechatronischen Maschinenenbau, Lehrstuhl für Magnetofluiddynamik, Mess- und Automatisierungstechnik
TU Dresden
George-Bähr-Straße 3
1062 Dresden
BRD
E-mail: adrian.lange@tu-dresden.de

Frank Ludwig
Institut für Elektrische Messtechnik und Grundlagen der Elektrotechnik
TU Braunschweig
Hans-Sommer-Str. 66
38106 Braunschweig
Germany
E-mail: f.ludwig@tu-bs.de

Michael Lentze
Deutsche Forschungsgemeinschaft e.V.
Kennedyallee 40
53175 Bonn
Germany
E-mail: Michael.Lentze@dfg.de

Stefan Lyer
SEON
Universitätsklinikum Erlangen
Glückstraße 10a
91054 Erlangen
Germany
E-mail: stefan.lyer@gmx.de

Andreas Menzel
Fakultät für Naturwissenschaften, Institut für Physik, Theorie der Weichen Materie / Biophysik
Otto-von-Guericke-Universität Magdeburg
Universitätsplatz 2
39106 Magdeburg
Germany
E-mail: a.menzel@ovgu.de

Gareth Monkman
Elektro- und Informationstechnik
OTH-Regensburg
Seybothstr. 2
93053 Regensburg
Deutschland
E-mail: gareth.monkman@oth-regensburg.de

Stefan Odenbach
Magnetofluiddynamik, Mess- und Automatsierungstechnik
TU Dresden
George-Bähr-Str. 3
1069 Dresden
Deutschland
E-mail: stefan.odenbach@tu-dresden.de

Chinmay Pabshettiwar
Institute for Computational Physics
University of Stuttgart
Allmandring 3
70569 Stuttgart
Germany
E-mail: cpabshettiwar@icp.uni-stuttgart.de

Harald Pleiner
Theory
Max Planck Institute for Polymer Physics
c/o Am Muehlborn 5
55218 Ingelheim
Germany
E-mail: pleiner@mpip-mainz.mpg.de

Marius Reiche
Mechanics of Compliant Systems Group
Technische Universität Ilmenau
Max-Planck-Ring 12
98693 Ilmenau
Deutschland
E-mail: marius.reiche@tu-ilmenau.de

Benoît Rhein
Department of Chemistry
University of Cologne
Greinstraße 04.Jun
50939 Cologne
Deutschland
E-mail: brhein@uni-koeln.de

Gerald Richwien
Department of Chemistry
University of Cologne
Greinstraße 04.Jun
50939 Cologne
Germany
E-mail: grichwie@smail.uni-koeln.de

Leonhard Rochels
Inorganic Chemistry
University of Duisburg-Essen
Universitätsstraße 7
45141 Essen
Deutschland
E-mail: leonhard.rochels@uni-due.de

Annette Schmidt
Chemistry Department
Universität zu Köln
Greinstr. 04.Jun
50939 Köln
Germany
E-mail: annette.schmidt@uni-koeln.de

Patrick Schütz
Institut für Physikalische Chemie
Universität Hamburg
Grindelallee 117
20146 Hamburg
Germany
E-mail: patrick.schuetz@uni-hamburg.de

Ioana Slabu
Institute of Applied Medical Engineering
RWTH Aachen
Pauwelsstr. 20
52074 Aachen
Germany
E-mail: slabu@ame.rwth-aachen.de

Andreas Tschöpe
Experimentalphysik
Universität des Saarlandes
Campus E2.6 02.Jun
66123 Saarbrücken
Germany
E-mail: andreas.tschoepe@uni-saarland.de

Thilo Viereck
Institut für Elektrische Messtechnik und Grundlagen der Elektrotechnik (EMG)
TU Braunschweig
Hans-Sommer-Straße 66
38106 Braunschweig
D
E-mail: t.viereck@tu-braunschweig.de

Thomas Wallmersperger
Maschinenwesen
IFKM/TU Dresden
George-Bähr-Str. 3c
1069 Dresden
Germany
E-mail: thomas.wallmersperger@tu-dresden.de

Maria Weißpflog
Institute of Physical Chemistry
University of Hamburg
Grindelallee 117
20146 Hamburg
Germany
E-mail: maria.weisspflog@uni-hamburg.de

Frank Wiekhorst
Metrology for Magnetic Nanoparticles
Physikalisch-Technische Bundesanstalt
Abbestr. 02.Dez
10587 Berlin
Germany
E-mail: frank.wiekhorst@ptb.de

Manuel Wolfschwenger
Biomedizinische Informatik und Mechatronik
UMIT Tirol
Eduard Wallnöfer Zentrum 1
6060 Hall in Tirol
Austria
E-mail: manuel.wolfschwenger@umit-tirol.at